ANL-7735

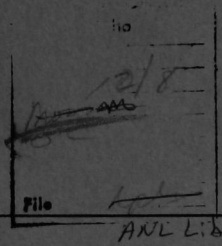

Argonne National Laboratory

CHEMICAL ENGINEERING DIVISION
FUEL CYCLE TECHNOLOGY QUARTERLY REPORT
APRIL, MAY, JUNE 1970

by

D. S. Webster, A. A. Jonke, G. J. Bernstein,
N. M. Levitz, R. D. Pierce,
M. J. Steindler, and R. C. Vogel

The facilities of Argonne National Laboratory are owned by the United States Government. Under the terms of a contract (W-31-109-Eng-38) between the U. S. Atomic Energy Commission, Argonne Universities Association and The University of Chicago, the University employs the staff and operates the Laboratory in accordance with policies and programs formulated, approved and reviewed by the Association.

MEMBERS OF ARGONNE UNIVERSITIES ASSOCIATION

The University of Arizona
Carnegie-Mellon University
Case Western Reserve University
The University of Chicago
University of Cincinnati
Illinois Institute of Technology
University of Illinois
Indiana University
Iowa State University
The University of Iowa
Kansas State University
The University of Kansas
Loyola University
Marquette University
Michigan State University
The University of Michigan
University of Minnesota
University of Missouri
Northwestern University
University of Notre Dame
The Ohio State University
Ohio University
The Pennsylvania State University
Purdue University
Saint Louis University
Southern Illinois University
The University of Texas at Austin
Washington University
Wayne State University
The University of Wisconsin

Printed in the United States of America
Available from
National Technical Information Service
U.S. Department of Commerce
Springfield, Virginia 22151
Price: Printed Copy $3.00; Microfiche $0.65

ANL-7735
Chemical Separations Processes
for Plutonium and Uranium

ARGONNE NATIONAL LABORATORY
9700 South Cass Avenue
Argonne, Illinois 60439

CHEMICAL ENGINEERING DIVISION
FUEL CYCLE TECHNOLOGY QUARTERLY REPORT
APRIL, MAY, JUNE 1970

by

D. S. Webster, A. A. Jonke, G. J. Bernstein,
N. M. Levitz, R. D. Pierce,
M. J. Steindler, and R. C. Vogel

July 1970

TABLE OF CONTENTS

LIST OF FIGURES

LIST OF TABLES

CHEMICAL ENGINEERING DIVISION

FUEL CYCLE TECHNOLOGY QUARTERLY REPORT

APRIL, MAY, JUNE 1970

ABSTRACT

Research and development efforts on Argonne National Laboratory's fuel cycle technology projects are reported for the period April through June 1970. Work was done in the following areas: (1) development of two conceptual designs for plants to declad 5 metric tons/day of LMFBR fuel in molten zinc, (2) construction of a fluid-bed pilot plant to continuously convert uranium-plutonium nitrate (in aqueous solution) to oxides, and laboratory experiments to identify the oxide products (i.e., phases) obtained by drop-denitration of uranium nitrate and U-20% Pu nitrate solutions at 300 to 600°C, (3) evaluation of X-ray fluorescence spectrometry as an in-line analytical method for determining the Pu/U ratio of oxide fuels, and consideration of X-ray diffraction measurement of the lattice parameter of single-phase (U,Pu) oxide as an in-line method of determining the oxygen content (O/M ratio) of oxide fuels; and (4) the development of a critically favorable centrifugal contactor for the efficient handling of plutonium from LMFBR fuels in the plutonium isolation steps of a solvent-extraction process.

Highlights of ANL investigations of liquid metal decladding since early 1968 are also presented.

FOREWORD

This quarterly report is the first in a series on LMFBR fuel recycle work at the Argonne National Laboratory. Its purpose is to keep the nuclear industry informed of our efforts, so that the programs can benefit from industrial views. Our original work on spent LMFBR fuels was directed toward two complete process alternatives for the decontamination and recovery of plutonium and uranium. Development of the fluoride volatility process ended in FY 1970. At the same time, emphasis in the pyrochemical process

was shifted to development of a head-end step that would be an alternative to the conventional shear-leach procedure. Currently, all work funded by the Division of Reactor Development and Technology (DRDT) of the AEC for study of LMFBR fuel reprocessing is aimed at a process which uses Purex solvent extraction to decontaminate and recover plutonium and uranium.

Design of a suitable shipping cask for fuel subassemblies was contracted to Aerojet General by DRDT. Oak Ridge National Laboratory is devising concepts for receiving and storing fuel and is also working on fuel shearing, roasting, and dissolving. WADCO Corporation (Westinghouse) will evaluate electrolytic decladding of fuel and will continue studies on dissolution of mixed oxides in nitric acid. Argonne is developing a method of decladding with molten zinc that offers advantages discussed in the text. Retention of iodine and fission gases released from fuel during the head-end step is being investigated by ANL and ORNL for their respective procedures.

Radiation degradation of solvent during extraction will be studied by WADCO, using very small centrifugal contactors. The general solvent extraction flowsheets are being devised by ORNL. A centrifugal mixer-settler of critically favorable geometry is under development at ANL to ease plutonium handling in the plutonium isolation cycles of solvent extraction; the work is described in this report.

Nitrate solutions of plutonium and uranium will be converted to oxides before fabrication into fuel elements. Oak Ridge is adapting the sol-gel process for the conversion to oxides and is exploring the use of sol-gel oxides in fabricated fuel. Argonne is adapting a fluid-bed denitration and reduction process for the conversion of nitrate solutions to oxides (see text), but is not fabricating fuel. The one ANL venture related to fuel fabrication is the development of in-line analytical methods described in this report.

These four ANL studies are summarized in the first section of this report and presented in detail in the following sections.

SUMMARY

I. LIQUID METAL DECLADDING OF REACTOR FUELS

The most difficult and costly aspect of LMFBR fuel processing in solvent-extraction fuel-recovery plants will probably be the head-end operations, which include fuel-subassembly handling, cladding removal, iodine removal, and introduction of fuel into the acid dissolution unit. Liquid-metal decladding is being developed as a head-end process to prepare discharged fast reactor fuels for introduction into fuel-recovery plants. Liquid-metal decladding is an attractive alternative to shearing discharged fuel into short lengths, and selectively leaching the exposed fuel from the stainless steel cladding with nitric acid. Although the shear-leach procedure is practiced with thermal reactor fuels, decladding of LMFBR fuels by shear-leaching would encounter problems related to the higher burnups, shorter cooling times, residual sodium, and high plutonium content of irradiated LMFBR fuels.

Decladding Kinetics

The rates and mechanisms of liquid-metal decladding have been studied at Argonne since early 1968. Highlights of decladding investigations at Argonne since that time are summarized in this report. Several experiments showed that stainless steel exposed to unagitated liquid zinc at 800°C disintegrates at rates ranging from two to four mils/min. This result indicates that immersion of LMFBR fuel subassemblies in zinc would accomplish complete cladding removal in less than 15 min and wrapper-tube disintegration in less than 1 hr.

The effect of irradiation on the rate of dissolution of stainless steel in zinc was studied with a type 304 stainless steel rod that had been irradiated in EBR-II. The irradiation level would correspond to a burnup of ∿2.2 at. % if LMFBR core fuel were exposed to this flux. The irradiated rod was dissolved in zinc along with several nonirradiated type 304 stainless steel rods of identical geometry to allow comparison of the dissolution rates of irradiated and nonirradiated alloys. The

dissolution rate for the irradiated stainless steel rod was about twice the rate for unirradiated rods; the irradiated rod was completely dissolved in about 30 min. This result suggests that irradiation enhances the kinetics of stainless steel dissolution in zinc.

It has been estimated that decladding solutions may accumulate as much as 1% sodium from sodium in failed fuel elements and on the exterior of fuel subassemblies. A series of experiments were conducted to determine the effect of sodium on zinc decladding of stainless steel. Decladding rates for runs with sodium present and absent did not differ significantly.

Stainless Steel Loading in Zinc

A study was performed of the nature of the cladding dissolution-disintegration process and of the possible loading of stainless steel in zinc. Experiments using metallographic, electron microprobe, X-ray, and thermal analysis techniques have indicated that: (1) the maximum solubility of stainless steel (i.e., solubility of all stainless steel constituents) in zinc is less than 8 wt %; (2) rapid disintegration of stainless steel continues after the zinc is saturated with chromium and iron; (3) loadings of 15 wt % (including suspended solids) are readily achieved, and the resulting mixtures are quite fluid with no evidence of settling of solids; and (4) effective separation of the zinc slurry from an oxide fuel bed appears to be feasible.

Engineering-Scale Experiments

Two experiments were conducted to study the processing of simulated fuel subassemblies loaded with unirradiated UO_2 pellets and fines. The subassemblies were subjected to a complete head-end processing operation including (a) dissolution of the stainless steel in molten zinc, (b) transfer of the zinc-stainless steel solution from the system, (c) vacuum distillation (from beneath a salt phase) of residual zinc associated with the UO_2, (d) reduction of the UO_2 pellets and fines to metal, and (e) separation of the Mg-Cu solution (which would contain plutonium in a process

run) from the precipitated uranium phase. The experimental results showed that the subassemblies had been completely dissolved, that effective phase separations were achieved without appreciable fuel losses, and that reduction efficiencies greater than 99% (possibly greater than 99.9%) were attained. It was concluded that no major problems exist in the interfacing of the various head-end operations.

Plant Concept Studies

During the report period, conceptual head-end plants processing 5 metric tons/day of LMFBR fuel have been designed for (a) zinc decladding followed by reduction of fuel oxides and (b) zinc decladding (to be followed by a voloxidation step under development at ORNL). Reduction and voloxidation are candidate process steps designed to effect the release of ^{131}I and other fission gases from irradiated LMFBR fuel prior to the nitric acid dissolution step of solvent extraction.

A capacity for the conceptual plant of about 5 metric tons/day was selected to establish a parallel with recent studies at ORNL. (However, liquid-metal decladding units of much lower capacity are also attractive.) The facility is assumed to operate 24 hr/day with a plant factor of 0.75. The plant can process 36 fuel subassemblies per operating day, which corresponds to about 10,000 subassemblies per year or about seventy-two 1000-MW(e) reactors serviced.

Liquid-metal decladding followed by reduction of the oxide fuel to metal appears to be a very flexible head-end process for nuclear fuels. Several equipment and process alternatives are promising.

As an example of a decladding-reduction plant, a single design was arbitrarily selected. The principal processing unit for the liquid-metal head-end step is a furnace with three operating stations. At each of the stations inside the furnace is a process vessel and all three vessels rest on the same rotatable platform. Decladding is performed at the first position, reduction of uranium and plutonium oxides to metal

at the second position, and dissolution of precipitated uranium metal at the third.

A conceptual plant has been designed to perform the decladding step (to be followed by voloxidation). The fuel subassemblies are immersed in liquid zinc contained in a large graphite vessel. When the stainless steel components of the subassembly dissolve, the fuel oxide drops into a perforated metal basket suspended in the liquid zinc and enclosing the bottom of the subassembly. The basket is lifted out of the zinc pool, the molten stainless steel-zinc is drained from the basket, and the declad fuel oxide is transported in the basket to the voloxidizer step of the aqueous process.

Preliminary equipment designs and descriptions of operations are presented for both plant-design alternatives. Reduction appears to be preferable to the voloxidation alternative because of its greater reliability in achieving efficient fission-gas removals and its better compatibility with the zinc decladding step.

II. CONTINUOUS CONVERSION OF U/Pu NITRATES TO OXIDES

The conversion of uranium nitrate and plutonium nitrate solutions to an oxide form suitable for the fabrication of fuel shapes is an important step in the LMFBR fuel cycle. Safe, reliable, and economic conversion appears possible using fluid-bed methods and is under investigation. The process, based on extensive fluid-bed technology, includes continuous fluid-bed denitration of solutions of one or more actinides. Denitration is followed by fluid-bed reduction for the case in which the denitration product contains uranium. For example, mixed UO_3-PuO_2 produced by denitration is reduced with hydrogen to UO_2-PuO_2. The powder product will be characterized and tested for suitability as fuel. An integrated program for laboratory studies and experimental work on a pilot engineering scale is in progress.

Laboratory Program

Features of the laboratory program and recent preliminary results include the following:

(1) Exploratory drop-denitration experiments at temperatures in the range from 300 to 600°C, first with uranium nitrate solutions alone, then with U-20% Pu nitrate solutions, and finally with plutonium nitrate alone. The oxide products were examined using several analytical techniques: X-ray diffraction, electron-microprobe examination, autoradiography, and microscopic examination. The major phase in the UO_3-20 wt % PuO_2 material made at 450°C was identified as gamma-UO_3; a possible minor phase was PuO_2. Plutonium nitrate solutions denitrated at 450°C and 300°C produced only PuO_2; product made at the higher temperature showed greater crystallinity. Electron-microprobe and autoradiographic examinations of mixed oxide powder prepared at 450°C indicated that the plutonium distribution in the uranium oxide matrix was rather uniform.

(2) Development and testing of a dissolution procedure for UO_3-PuO_2 material produced by denitration. This procedure is of interest

for the pilot-scale studies in which the denitration products will be redissolved and recycled to minimize plutonium inventory requirements. Dissolution of mixed oxides produced by drop-denitration at several temperatures was carried out in nitric acid at 95-120°C and to final actinide concentrations of 0.35 and 1.5M. The data indicated that (a) oxide produced at the lowest temperature, 300°C, was easiest to dissolve, (b) the oxide dissolution rate was unaffected by the dissolution temperature, (c) the dissolution rate was unaffected by the final actinide concentration, when dissolution was with 16M nitric acid, and (d) the fraction of plutonium dissolved was greater with concentrated acid; also the rate of plutonium dissolution was significantly higher for UO_3-20 wt % PuO_2 material than for PuO_2 alone--~99% as compared with 30-50% in 5 hr.

Engineering Program

A fluid-bed pilot plant was constructed in an existing 3- by 4-module glovebox. The central unit is a 4-in.-dia fluid-bed denitrator with integral filters, and is considered to be critically safe for uranium-20% plutonium systems. Auxiliaries include a feed make-up system, fluidizing-gas preheater, an off-gas condenser and condensate receiver, a demister, and a high-efficiency (AEC-type) filter for further off-gas cleanup. All process vessels are of stainless steel. The final off-gas and the room and glovebox air are scrubbed and passed through AEC-type filters before being discharged to the building stacks. Sorption of NO_2 and condensation of nitric acid in a condenser was selected as the off-gas treatment in preference to alternative methods after an examination of the factors involved. Similarly, batch preparation rather than continuous preparation of feed solution was chosen.

A plastic mock-up of the 4-in.-dia denitrator has also been constructed to study selected phases of column operation. With sintered alumina as a stand-in for a fluidized bed of actinide materials, the response of differential pressure instrumentation was examined on (a)

the primary sintered metal filters and (b) the fluidized bed itself. Data showed that failure of the filters by plugging or rupture would be detected. The Δp traces pertaining to the bed were not sufficiently sensitive to changes in the particle-size distribution of the bed to serve as a monitoring method, but a continuous monitor for particle size distribution would be of extreme value, and its development should be pursued.

A separate study showed that a side takeoff for product withdrawal would be preferable to an internal overflow line.

III. IN-LINE ANALYSIS IN FUEL FABRICATION

The development of in-line nondestructive methods for analysis of critical fuel properties should lower fuel fabrication costs for the large number of fuel subassemblies required in the LMFBR program. The specifications of fuel properties (and the associated precisions) for the Fast Fuel Test Facility (FFTF) project are discussed and considered as the starting criteria in evaluating analytical methods to be developed. Some relaxation of the present rigorous specifications for fuel properties may occur as additional information on the relationship between fuel properties and performance is obtained from irradiation experiments.

In the evaluation of X-ray fluorescence spectrometry as an analytical method for determining the Pu/U ratio, U-Th oxides are being utilized because of the identical atomic number relationship of Pu/U and U/Th. Recent experiments have demonstrated this approach to be feasible.

The utilization of X-ray diffraction measurement of the lattice parameter of single-phase cubic (U, Pu) oxide to determine the oxygen content (O/M ratio) of the oxide is reviewed. Existing data on analytical methods for determining O/M ratios and the lattice parameters of single-phase $(U,Pu)O_{2\pm x}$ are summarized.

IV. ADAPTATION OF CENTRIFUGAL CONTACTORS IN LMFBR FUEL PROCESSING

Development of a centrifugal contactor with a large length-to-diameter ratio is being studied to extend centrifugal-contactor design to a configuration suitable for the plutonium isolation steps in the solvent extraction of LMFBR fuels. The advantages sought are a geometrically favorable design for criticality control, reduced radiation damage to solvent, and increased ease of operation.

The basic contactor design being studied is patterned after units developed at the Savannah River Laboratory. In this type of contactor, solvent and aqueous phases are fed into a chamber at the bottom of the contactor where they are mixed by a rotating paddle. The chamber also acts as a centrifugal pump and discharges the mixed phases into a hollow rotor bowl located directly above the mixing chamber and mounted on the same shaft as the paddle. As the phases move upward, they are separated by centrifugal force and are discharged through ports located near the top of the rotor.

The first unit being built for evaluation has a 4-in.-dia rotor bowl which has a 12-in.-long settling zone and is designed to operate at speeds up to about 3600 rpm. The anticipated settling capacity is about 12 gal/min. In comparison, the Savannah River production contactors currently in use have 10-in.-dia rotor bowls with 13-in.-long settling zones operating at 1750 rpm, and settling capacities of 40-60 gal/min.

Capacity data obtained from tests of the ANL unit will be integrated with data from several sizes of contactors tested at Savannah River and will be used as a basis for the design of a high-capacity contactor of critically favorable geometry. Such contactors will be particularly useful for processing short-cooled fuel containing high concentrations of plutonium.

Additional tests will be made with contactors having larger length-to-diameter ratios and other variations in the basic design which will simplify construction and operation.

A test facility has been built for testing experimental contactors with various organic and aqueous streams. The facility is equipped with a variable-speed drive motor for operating the contactor over a range of speeds and with pumps and flow meters suitable for handling feed streams up to 20 gal/min each.

CHEMICAL ENGINEERING DIVISION

FUEL CYCLE TECHNOLOGY QUARTERLY REPORT

APRIL, MAY, JUNE 1970

I. LIQUID METAL DECLADDING OF REACTOR FUELS

(R. D. Pierce, W. J. Walsh, I. O. Winsch)

A. INTRODUCTION

The reference fuel recovery method for liquid-metal-cooled fast breeder reactors (LMFBRs) of the future is a modified shear-leach process followed by solvent extraction currently under development at ORNL.[1] The most difficult and costly aspect of LMFBR fuel processing will probably be the head-end operations, which include fuel-subassembly handling, cladding removal, iodine removal, and introduction of fuel into the acid dissolution unit. Liquid-metal decladding processes under development at Argonne[2] provide an attractive alternative to shearing the fuel into short lengths and selectively leaching the exposed fuel from the stainless steel cladding with nitric acid. The shear-leach procedure is practiced with light-water-moderated thermal reactor (LWR) fuels, but decladding of LMFBR fuels by shear-leaching would encounter problems related to the higher burnups, shorter cooling times, residual sodium, and high plutonium content of irradiated LMFBR fuels.

Designs of fast reactor fuel subassemblies are still in a period of evolution and development, but the early LMFBR fuels will consist of mixed uranium and plutonium oxides jacketed in stainless steel tubes. A core fuel subassembly typically is expected to consist of about 200 to 300 fuel elements closely packed in a hexagonal stainless steel wrapper tube. A subassembly is expected to be about 6 in. across the flats and 12-18 ft long, with a central fuel region about 6 ft long. Although head-end processing requirements are presently uncertain, it is clear that the high specific power and burnup levels of LMFBR fuels will present several for-

---

[1] W. E. Unger et al, "Aqueous Processing of LMFBR Fuels," Progress Reports No. 1-13, USAEC Reports ORNL-TM-2552, 2585, 2624, 2650, 2671, 2710, 2748, 2764, 2795, 2819, 2871, 2918, and 2949 (March 1969 to March 1970).

[2] R. C. Vogel, M. Levenson, E. R. Proud, and J. Royal, "Chemical Engineering Division Annual Report--1968," USAEC Report ANL-7575, pp. 28-31 (1969).

midable head-end processing problems.[3] LMFBR fuels may be irradiated to burnups up to 100,000 MWd/ton at specific powers as high as 175 kW/kg and may be allowed to decay for only 30 days; this is in contrast to LWR fuels, which may be irradiated to less than 40,000 MWd/ton at about 35 kW/kg and allowed to decay for 150 days or longer. The localized heat emission of LMFBR fuels is very high, creating heat-dissipation problems during handling and processing operations.

High concentrations of radioactive iodine, xenon, and krypton in spent LMFBR fuel will present serious problems in handling and disposing of the waste-gas effluent from reprocessing operations. The quantity of ^{131}I (especially potent as a biological hazard) in 30-day cooled LMFBR core fuel will be 400,000 times the quantity in 150-day cooled LWR fuels. To avoid excessive emissions of ^{131}I to the environment, head-end operations must be performed in a sealed cell and fission gas must be efficiently removed prior to the nitric acid dissolution step.

The presence of sodium (not normally encountered in LWR fuels) in failed fuel elements would present cleaning and fuel-dissolution problems since sodium can react explosively with the nitric acid used in a dissolution step. In addition, the higher plutonium content of LMFBR fuel presents more severe criticality problems.

Alternatives to shear-leach head-end processing of nuclear fuels have been studied at Argonne since early 1968.[2,4] Major emphasis has been on the development of the zinc decladding step of the Salt-Transport Process[5] as a head-end for aqueous processing. The highlights of earlier zinc

---

[3] C. D. Watson et al, "Proceedings of the 16th Conference on Remote Systems Technology," pp. 19-38, Amer. Nucl. Soc. (1969).

[4] R. C. Vogel, L. Burris, A. D. Tevebaugh, D. S. Webster, E. R. Proud, and J. Royal, "Chemical Engineering Division Annual Report--1969," USAEC Report ANL-7675 (1970) (in press).

[5] R. K. Steunenberg, R. D. Pierce, and I. Johnson, "Symposium on Processing of Nuclear Fuels," Nucl. Metal., Vol. 15, pp. 325-335, USAEC Report CONF-69081 (1969).

decladding investigations at Argonne are presented in this report, along with current work, as background for this series of progress reports. Other head-end alternatives studied at Argonne include antimony-copper decladding[6] (reported here briefly) and direct melting of stainless steel[7,8] (not reported here).

In liquid-metal decladding, cladding is removed by immersing a discharged fuel subassembly (probably after cropping the bottom) in molten zinc. The zinc dissolves the stainless steel components (both the subassembly supporting members and the cladding) but does not react with the fuel oxides. This procedure avoids mechanical disassembly, handling of individual fuel elements, and shearing of fuel hardware by remote control from behind thick shielding, which would have to be done if the shear-leach alternative were selected. Other advantages of liquid-metal decladding include (1) efficient removal of iodine and other volatile fission products, (2) relative ease of dissipation of fission-product heat, (3) elimination of the requirement for separate sodium-removal steps, (4) discharge of all process waste streams (except Xe and Kr) as solids having good heat transfer properties, (5) collection of xenon and krypton in an inert gas (containing ~50% Xe plus Kr) that can be stored, (6) absence of effective neutron-moderating elements, and (7) process simplicity and flexibility.

The principal disadvantages of liquid-metal decladding are the lack of industrial experience in the use of refractory metals and graphite as materials of construction, and the large quantities of reagent zinc discharged as waste. Refractory metals and graphite are compatible with

---

[6] M. Payrisaat, J. G. Wurm, "Decladding of UO_2/PuO_2/Stainless Steel Fast Reactor Fuels by Liquid Metals," EAES Symposium, Mol, Belgium (1968).

[7] K. Hartley, British Patent G6 (G21) N977566 (1963).

[8] G. P. Novoselov and A. I. Ageenkov, "Thermal Method of Decladding Stainless Steel Canned Fuel Elements," Preprint, Fuel Processing Symposium, Mol, Belgium (1966).

liquid zinc and molten salts; equipment fabricated of these materials have long lives but their cost is a significant portion of the processing cost. For each ton of fuel processed, about 15 ft^3 of zinc is discharged to waste. Solid zinc is an ideal waste form, and the reagent and waste-disposal costs are not large. If desired, recovery of the zinc may be achieved by a zinc-vaporization process.

Liquid-metal decladding processes appear to provide relatively simple and inexpensive techniques for accomplishing head-end objectives. Conceptual design studies show that a single liquid-metal decladding unit is capable of processing 5 tons/day of LMFBR fuel. However, smaller head-end units may prove advantageous and appear to be equally feasible.

In a society becoming increasingly concerned with protecting the environment, the reduction of radiological hazards to very low levels may become a necessity. In the event that shipping of short-cooled LMFBR fuel elements is not permitted because of more restrictive safety regulations in the future, liquid-metal decladding and reduction performed on-site would allow efficient recovery of the plutonium in a copper-base solid alloy possessing good heat-transfer properties. Since this treatment results in the most hazardous fission products being removed, immediate shipment to a large central aqueous-processing plant may be possible.

B. STAINLESS STEEL LOADING IN ZINC

Based on an analysis of the binary phase diagrams of Zn-Fe, Zn-Cr, and Zn-Ni, it was estimated that the zinc would become saturated with chromium and iron at a loading of about 7-10 wt % stainless steel. A series of four experiments was made to investigate the maximum loading of stainless steel in zinc at 800-850°C and to study the effects of loading on the dissolution rate. These experiments involved heating 4.8 kg of zinc and 0.1 kg of salt to a steady-state temperature in the range 800-850°C and introducing into the melt type 304 stainless steel rods (3/8-in. dia by 1 in.) equivalent to 15 wt % loading. The systems were agitated mildly to promote homogenization of the zinc-stainless steel solution, and filtered samples were taken sequentially to monitor the rate and extent of dissolution. In all four experiments, the iron and chromium concentrations of the filtered

samples of the liquid-metal phase rose rapidly to about 5.8 wt % and 1.0 wt %, respectively, and remained essentially constant thereafter. About one-half of the stainless steel charged in each experiment was in solution in the zinc; however, examination of the frozen ingots at the end of the experiments showed that the rods had completely disintegrated. Sections of the ingots were metallographically examined and found to contain suspensions of finely divided grains of alpha-iron containing zinc and chromium in solid solution.

A separate study of the nature of the dissolution-disintegration process was performed by Myles[4] who used metallographic, electron microprobe, X-ray, and thermal analysis techniques. Myles found that the dissolution-disintegration process begins with penetration of liquid zinc into the grains of stainless steel and with the preferential diffusion of nickel from stainless steel into zinc. Iron and chromium were observed to enter the zinc at rates lower than that for nickel. As the stainless steel is depleted of nickel, the structure of the austenitic gamma phase transforms into the ferritic alpha phase. Numerous cracks form rapidly and alpha-iron grains (containing chromium and zinc in solid solution) dislodge and are carried away in "rivers" of zinc into the bulk zinc phase. The entire process was observed to be rapid, explaining the high decladding rates which occur in the absence of external agitation. Myles observed no tendency of alpha-iron grains to settle in zinc solutions for static holding periods of several days.

These experiments have led to the following conclusions: (1) the maximum solubility of stainless steel in zinc is less than 8 wt %; (2) rapid disintegration of stainless steel continues after the zinc is saturated with chromium and iron; (3) loadings of 15 wt % (including the suspended solids) are readily achieved, and the resulting mixtures are quite fluid with no evidence of settling of solids; and (4) effective separation of the zinc slurry from an oxide fuel bed appears to be feasible.

C. DECLADDING KINETICS

The rates and mechanisms of liquid-metal decladding have been studied at Argonne since early 1968.[2,4,5] Several experiments have shown

that stainless steel surfaces exposed to unagitated liquid zinc at 800°C disintegrate at rates ranging from 2 to 4 mils/min.[4] This result indicates that LMFBR fuel subassemblies immersed in zinc would experience complete cladding removal in less than 15 min and that wrapper-tube disintegration would occur in less than one hour.

A series of three experiments was conducted to determine the relative rates of dissolution in zinc of Zircaloy-2 and stainless steel types 304 and 316 at 800°C. An additional experiment involving dissolution of type 304 stainless steel in Sb-18 at. % Cu at 900°C was performed. In each zinc test, a 4.5-in.-dia baffled tungsten crucible was charged with 3.67 kg of zinc and 100 g of salt (which formed a cover layer and retarded zinc vaporization). The system was brought to a steady-state temperature of 800°C, and a disc (attached rigidly to the bottom of a 2-in.-dia agitator and encased in tantalum except for a 3/4-in.-dia circular area of the bottom surface that was in direct contact with the zinc) was lowered into the melt. The tantalum enclosures prevented the changing configuration of the dissolving specimen from altering the mixing characteristics and also provided a fixed, known surface area in the early stages of dissolution. The agitator was rotated at 350 rpm to ensure homogeneity of the liquid metal for sampling. Filtered samples of the liquid-metal solution were taken during dissolution. The results of these four tests are given in Fig. 1. The slowest dissolution was observed for type 304 stainless steel in zinc. Since this system had previously been demonstrated on an engineering scale to possess a satisfactory decladding rate,[2] it is clear that the other three systems tested would also have practical decladding rates.

An experiment to test the effect of irradiation on the rate of dissolution of stainless steel in zinc utilized a type 304 stainless steel rod that had been irradiated in EBR-II from August 29, 1965, to January 22, 1966, at a flux of 4.9×10^{13} neutrons/(cm^2)(sec)(MW) with an average neutron energy of ∿400 keV. This irradiation would correspond to a burnup of ∿2.2 at. % if LMFBR core fuel were exposed to this flux. The irradiated rod was dissolved along with several nonirradiated type 304 stainless steel rods of identical geometry to allow comparison of the dissolution rates of

Figure 1

Dissolution of Cladding Materials by Liquid Zinc and Antimony-Copper

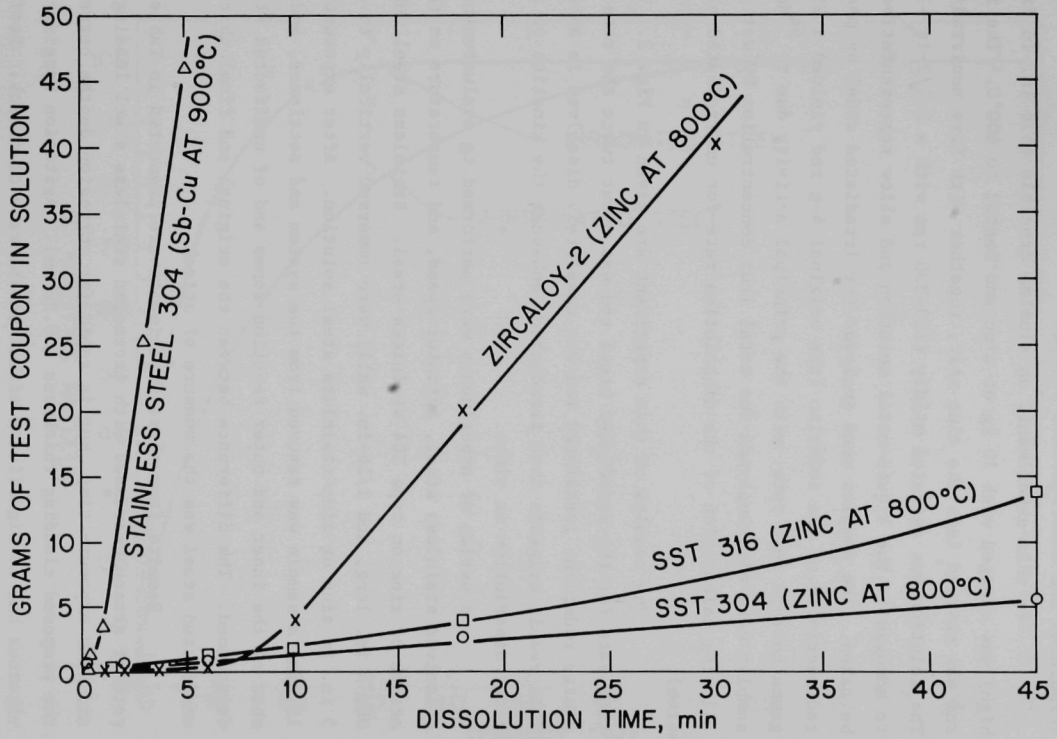

irradiated and nonirradiated alloys.

In this experiment, an alumina crucible (5.6 in. in dia by 12 in. high) was charged with 10 kg of zinc and heated to 800°C. The irradiated rod was charged into the zinc melt, together with five nonirradiated rods. The solution was agitated mildly (150-300 rpm with a 2 1/2-in.-long paddle) to homogenize the liquid-metal solution and allow representative samples to be taken. The samples were analyzed for irradiated steel by measuring the radioactivity of the solution (the original 4-g rod yielded a 25-R beta-gamma contact dose rate, with the principal activity due to ^{54}Mn). The samples were also analyzed for total iron concentration by wet chemistry, allowing calculation of the dissolution rate for unirradiated stainless steel.

The results of this experiment are given in Fig. 2. The dissolution rate for the irradiated steel rod was about twice the rate for unirradiated rods; the irradiated rod was completely dissolved in about 30 min. This result suggests that irradiation enhances the kinetics of stainless steel dissolution in zinc.

A series of experiments were performed to evaluate the effects of dissolved stainless steel, agitator speed, and temperature on the rate of attack of zinc on type 304 stainless steel. Stainless steel tubes (3/4-in. OD, 4 in. long, and 1/16-in. wall) were immersed vertically to a depth of 3 in. in zinc or zinc-stainless steel solution. After exposure from 1 to 15 min, a sample was removed from the system and sectioned, and the thickness of the inner and outer reaction zones and of unaffected steel was determined. The difference between the original and final thickness of unaffected steel was the measure of attack.

Results from these experiments are presented in Table 1. The rate of attack decreases with increased stainless steel loading of the zinc and with exposure time, but is rapid for corrosion depths corresponding to the proposed cladding thickness ($\sim$0.38 mm). Agitation ranging from none to vigorous had no significant effect on the rate of attack. Decreasing the melt temperature to 728°C decreased the rate of attack by a factor of 4 or 5.

Figure 2

Zinc Dissolution Kinetics of Irradiated and Unirradiated Type 304 Stainless Steel Rods

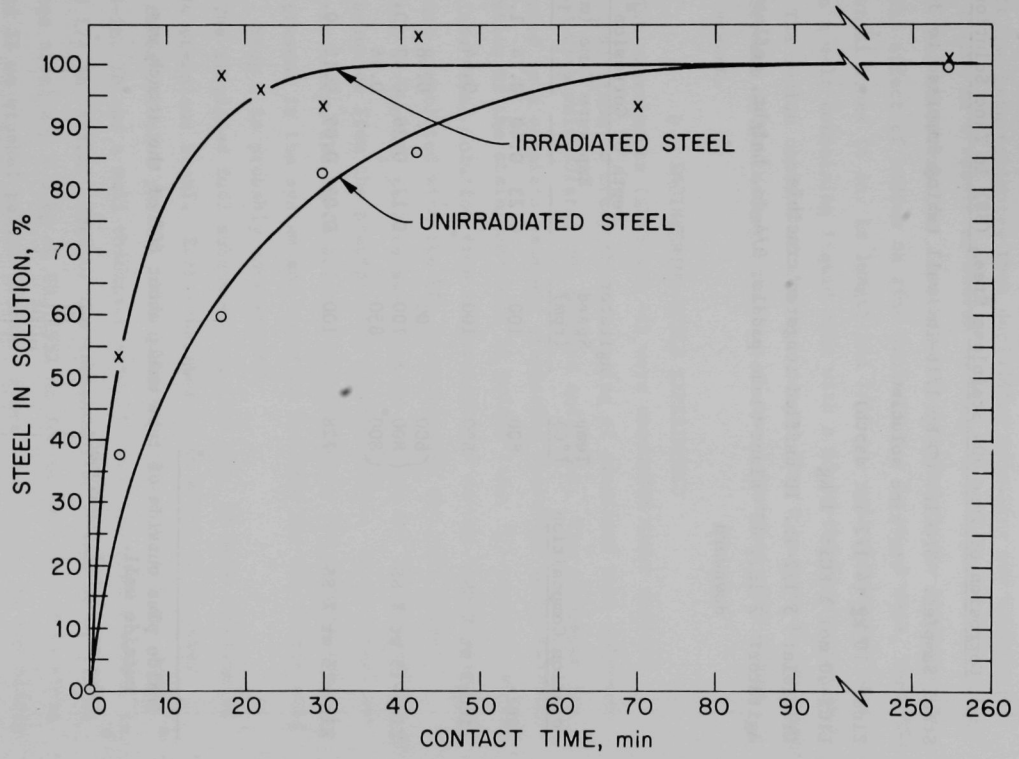

Table 1

Corrosion of Type 304 Stainless Steel (SS) in Zinc Solutions

Steel Samples: 3/4-in. OD by 1/16-in. wall tubing immersed to 3-in. depth in zinc solution

Zinc: 10 kg (4 1/2-in. depth)

LiCl-40 mol % KCl: 1 kg

Crucible: 5 1/2-in. ID baffled tungsten crucible

Agitator: 2 in., 45° slant-blade paddle, 3/4-in. height, deflecting downward

Solution Composition	Temp (°C)	Agitator Speed (rpm)	Depth of Corrosion[a] (mm) Exposure Time (min) 1	2	5	10	15
Zinc	800	100	0.23	0.40	0.74	1.20	1.60[b]
Zinc-3 wt % SS	800	100			0.64		
Zinc-15 wt % SS	800	0			0.48		
	800	100	0.17	0.26	0.49	0.75	0.97
	800	850			0.46		
Zinc-15 wt % SS	728	100	0.03	0.09	0.12	0.14	

[a] Inside plus outside of tube wall; about 60% of the attack was on the outside wall.

[b] Tube completely consumed.

It has been estimated that decladding solutions may contain as much as 1% sodium as a result of sodium in failed fuel elements and on the exterior of fuel subassemblies. A series of experiments was conducted to determine the effect of sodium on zinc decladding. In these runs, type 304 stainless steel tubes (4 in. in length and 1/16-in. wall thickness) were immersed in a melt containing liquid zinc with a mixed-chloride cover salt at 800°C. The sodium content of the zinc ranged from 0 to 1 wt %. No significant difference in decladding rates was observed for runs with sodium present or absent.

D. ENGINEERING-SCALE EXPERIMENTS

Two experiments (ZD-3 and -4) were conducted under similar processing conditions to study the processing of simulated fuel subassemblies loaded with unirradiated UO_2 pellets and fines. The subassemblies were subjected to a complete head-end processing operation which included (a) dissolution of the stainless steel in molten zinc, (b) transfer of the zinc-stainless steel solution from the system, (c) vacuum distillation of residual zinc associated with the UO_2 (from beneath the salt phase), (d) reduction of the UO_2 pellets and fines to uranium and (e) separation of the Mg-Cu solution from the precipitated uranium phase. In an actual reprocessing facility, the Mg-Cu solution would contain the bulk of the plutonium present in the system and would be the feed for the nitric acid dissolver. Step c is probably unnecessary.

The simulated fuel subassemblies (see Fig. 3) were constructed of type 304 stainless steel. Each consisted of an array of 13 tubes welded to three circular plates. The tubes were about 12 1/2 in. long, with a 3/8-in. ID and a wall thickness of 0.035 in. The plates were 4 in. in dia and 1/4 in. thick. Each of the subassemblies consisted of 2.7 kg of stainless steel and 2.5 kg of UO_2 (95% as 3/8-in.-dia by 1/2-in.-long pellets and 5% as crushed pellet fines). Fines were loaded at the middle region of each tube. A stainless steel holding rod (33 in. long by 5/8 in. in diameter) was welded to the top plate of each subassembly for positioning the subassembly in the liquid zinc.

Figure 3

Simulated Fuel Subassembly

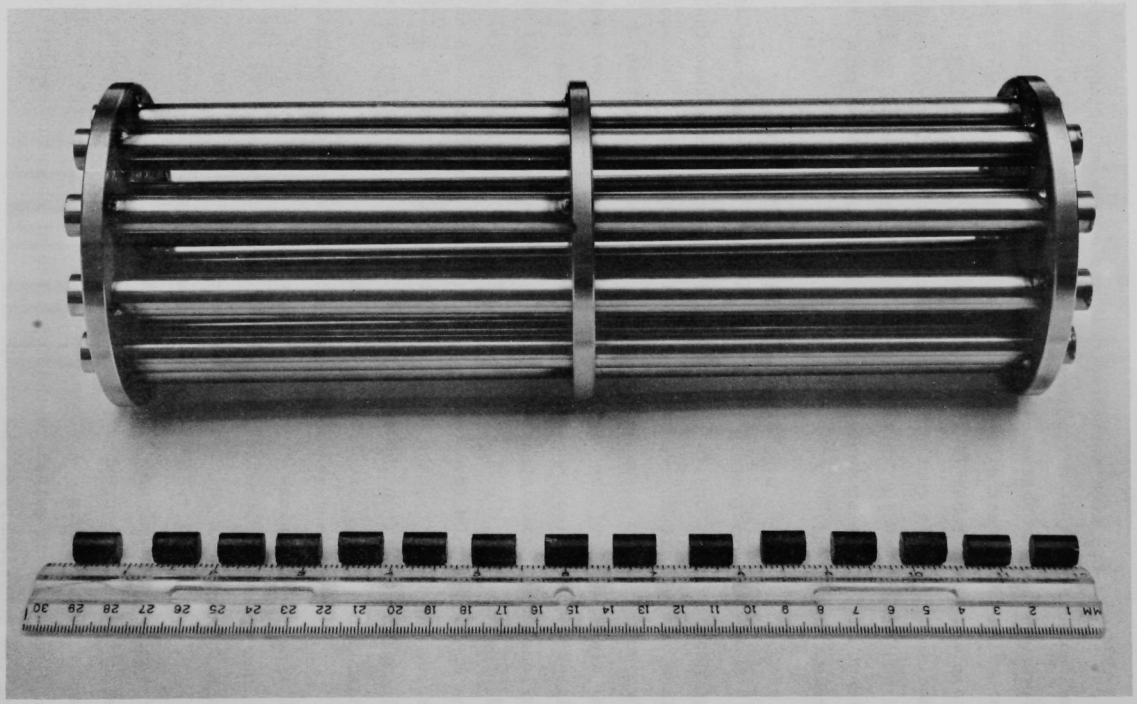

The decladding experiments were conducted in a 9 3/8-in. ID pressed-and-sintered tungsten crucible contained in a furnace vessel having an argon atmosphere. The crucible was loaded with 84.5 kg of zinc to provide a depth of liquid metal of 14 in. About 6 kg of $CaCl_2$-20 mol % CaF_2 (which when melted formed a layer about 2 in. thick) was charged to the crucible to retard vaporization of the zinc and to collect UO_2 fines. The system was then heated to 800°C, and a simulated subassembly was completely submerged in the melt. After about 30 min of contact, the tubing had been completely dissolved, but the holding rod and plates were relatively intact. An additional 7 hr of contact (with moderate agitation) was employed to ensure dissolution of all of the stainless steel. Filtered samples of the zinc-stainless steel solution were taken to determine the rate of dissolution in both runs. The results are presented in Fig. 4. The data indicate that the 0.035-in. tubing was dissolved in less than 30 min, but about 4 hr was required for dissolution of the spacer plates. The cladding and the stainless steel hardware dissolved in these experiments were considerably more massive than that which will be encountered in LMFBR fuel processing. For example, the Atomics International Follow-On Design[9] specifies 0.015-in. cladding thickness and 0.100-in.-thick wrapper tube.

Most of the zinc-stainless steel solution was removed through a transfer line at the conclusion of the decladding step in each run. The zinc-stainless steel ingots were subsequently dissolved in nitric acid. Analysis of the acid solution for ZD-4 showed that the ingots contained very little entrained UO_2 ($\sim$0.01% of the uranium charged).

After the bulk of the zinc-stainless steel solution had been transferred from the crucible, a water-cooled condenser was connected to the furnace vessel through the opening also used for the transfer line. Gas flowed out of the furnace, then through the condenser and to the vacuum system. The condenser consisted of a horizontal section of steel tube

---

[9] "Atomics International LMFBR Follow-On Study - Task II Report," Vol. 1, 2, and 3, USAEC Report, AI-AEC-12791 (1969)

Figure 4

Kinetics of Simulated Fuel Subassembly Dissolution in Molten Zinc

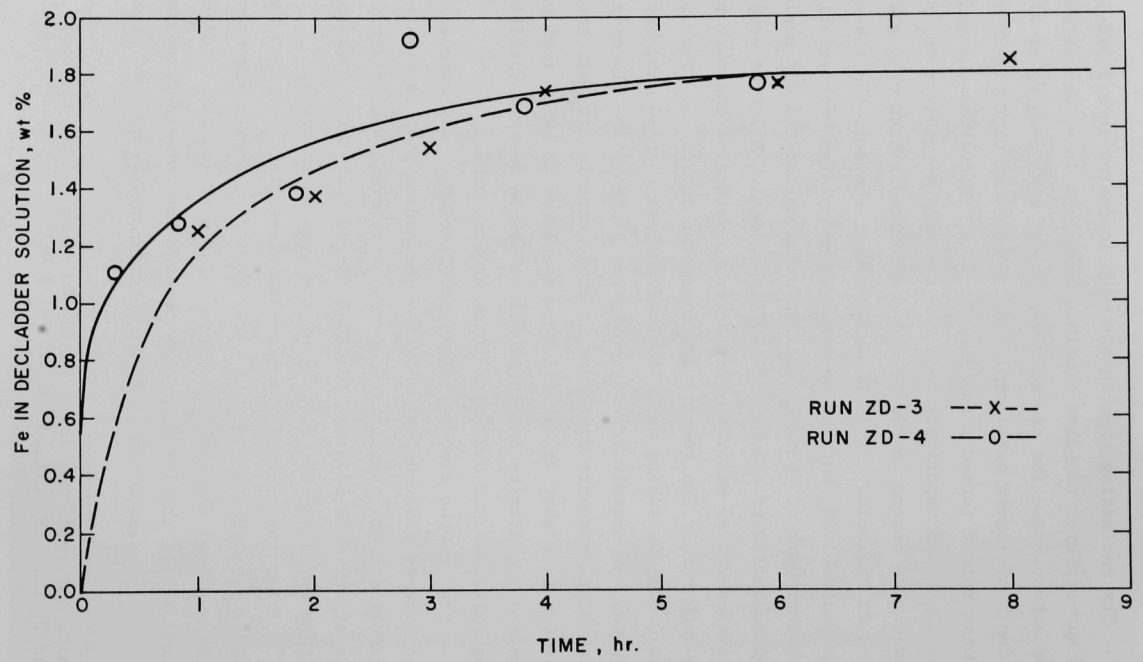

having internal flow baffles and external cooling coils. When the system was evacuated through the condenser, a high rate of zinc vaporization from the heel was observed. The zinc vapors had passed through the 2-in.-deep salt layer. The crucible contents were maintained at about 800°C throughout the vaporization step.

About 2.3 kg and 4.0 kg of zinc were collected by distillation in Runs ZD-3 and ZD-4, respectively. At the rates of distillation employed, and without provision for deentrainment, there was some salt entrainment, but uranium entrainment was low (<0.1% of the uranium).

Following the zinc-distillation step, the UO_2 in the crucible was reduced to metal with Mg-42 at.% Cu-3 at.% Ca. Reduction efficiencies greater than 99% were achieved in both experiments. A sludge, attributed to uranium nitride formation, was present with the precipitated uranium in Run ZD-3. Run ZD-4 was conducted by a technique that prevented contamination of the atmosphere, and no sludge was observed.

It was concluded that (a) the subassemblies had been completely dissolved, (b) effective phase separations were achieved without appreciable fuel losses, (c) reduction efficiencies greater than 99% (possibly greater than 99.9%) were attained, and (d) no major problems exist in the interfacing of the head-end operations.

E. PLANT CONCEPT STUDIES

Conceptual head-end plants processing 5 tons/day of LMFBR fuel have been designed, during the report period, for (a) zinc decladding followed by reduction of fuel oxides, and (b) zinc decladding (to be followed by the voloxidation step under development at ORNL).[3] Reduction and voloxidation are candidate process steps designed to effect the release of ^{131}I and other fission gases from irradiated LMFBR fuel prior to nitric acid dissolution. The reduction alternative appears to be preferable because of higher process reliability in achieving efficient fission-gas removals and relative ease in interfacing with the zinc decladding step.

LMFBR fuel-subassembly designs and the aqueous-processing steps are still in a period of evolution and development, and head-end processing

requirements are presently uncertain. In order to provide a basis for the plant design, a single set of processing conditions was selected.

A plant capacity of about 5 tons/day was selected to establish a parallel with recent processing studies at ORNL.[1] The facility is assumed to operate 24 hr/day with a plant factor of 0.75. The plant can process 36 fuel subassemblies per operating day, which corresponds to about 10,000 subassemblies per year; and, in the case of the Atomics International (AI) Conceptual Design,[9] about seventy-two 1000-MW(e) reactors can be serviced and 4.8 tons/day of fuel processed. It is assumed that core fuel and axial and radial blankets will be processed together in the head-end unit since the ORNL separations processes[1] being developed are based on homogenized fuel input. The head-end plant could operate somewhat more efficiently if the radial blanket were processed in a separate campaign in the same facility.

The Atomics International Follow-On Study "Final Reference Design"[9] was selected as an example of LMFBR fuel charged to a liquid-metal decladding process. The subassemblies are each 15 ft long and 5.667 in. across the flats. The core subassemblies each contain 217 nonvented fuel elements, which have a core region 42.8 in. long and upper and lower axial blankets of 15 and 12 in., respectively. The bottom hardware is cut off prior to processing, and the upper hardware remains unimmersed during decladding.

1. Zinc Decladding-Reduction Alternative

Liquid-metal decladding followed by reduction appears to be a very flexible head-end process for nuclear fuels. Several equipment and process alternatives are promising.

To provide an example of a decladding-reduction plant, the following procedure and design were arbitrarily selected:

Fuel subassemblies are shipped, unloaded, and stored in a pool (probably under water but liquid metals are also being considered) and the bottoms are cropped. An array of three subassemblies is raised into a transfer turret for transport. Forced-gas cooling may be employed to prevent excessive cladding temperatures during transfer to a furnace with three operating stations, which is the principal processing unit for the liquid-metal head-end step. A concept of this unit is represented in plan

and elevation views in Fig. 5 and 6. At each of three positions inside the furnace, resting on a rotatable platform, is a process vessel. Decladding is performed at one position, reduction of uranium and plutonium at the second position, and uranium dissolution at the third.

After the transfer turret is affixed to the furnace at the decladding station, gates are opened at the decladding port and in the transfer turret, and the fuel is lowered through the cover salt until it is immersed to a depth of a few inches in the zinc. The system is held at 800°C throughout a run. After the bottom cladding of the fuel elements has dissolved and the fission gases have vented (about 15 min), the fuel is lowered so that the zinc covers the fuel completely. For the case of vented fuel elements, the above step may be omitted and instead the subassemblies may be lowered immediately to a position that immerses the fuel zone in zinc. A period of about one hour is then allowed to digest the cladding. Next, the zinc-steel mixture is pressure-transferred out of the process vessel through a transfer line. A maximum pressure of about 20 psi is required for zinc transfer. This zinc is recycled twice through the decladding step before being either discarded or recovered from the waste steel by vacuum distillation. The salt remains in the vessel during this step.

After the zinc is removed, the three vessels in the head-end furnace are rotated (clockwise 120°, see Fig. 5). Prior to rotation, the vessels (on the platform) must be lowered about 7 ft so that they are not obstructed during rotation by agitators and transfer lines (see Fig. 6). After rotation, the vessels are raised to the operating level. The mechanisms and seals for raising, lowering, and rotating these vessels are below the heated zone.

Once rotated to the reduction position, a process vessel is charged with Mg-Cu-Ca alloy and additional salt in preparation for the reduction step. Agitation for about 90 min promotes reduction of fuel oxide. At the end of this period, agitation is stopped and the metal and salt phases separate. The salt phase is pressure-transferred out of the vessel as waste, and the Mg-Cu-Pu solution ($\sim$10 wt % plutonium) is pressure-transferred from the vessel as recovered product. Maximum pressures of about 5 and 12 psi,

Figure 5

Head-End Processing Unit - Plan View

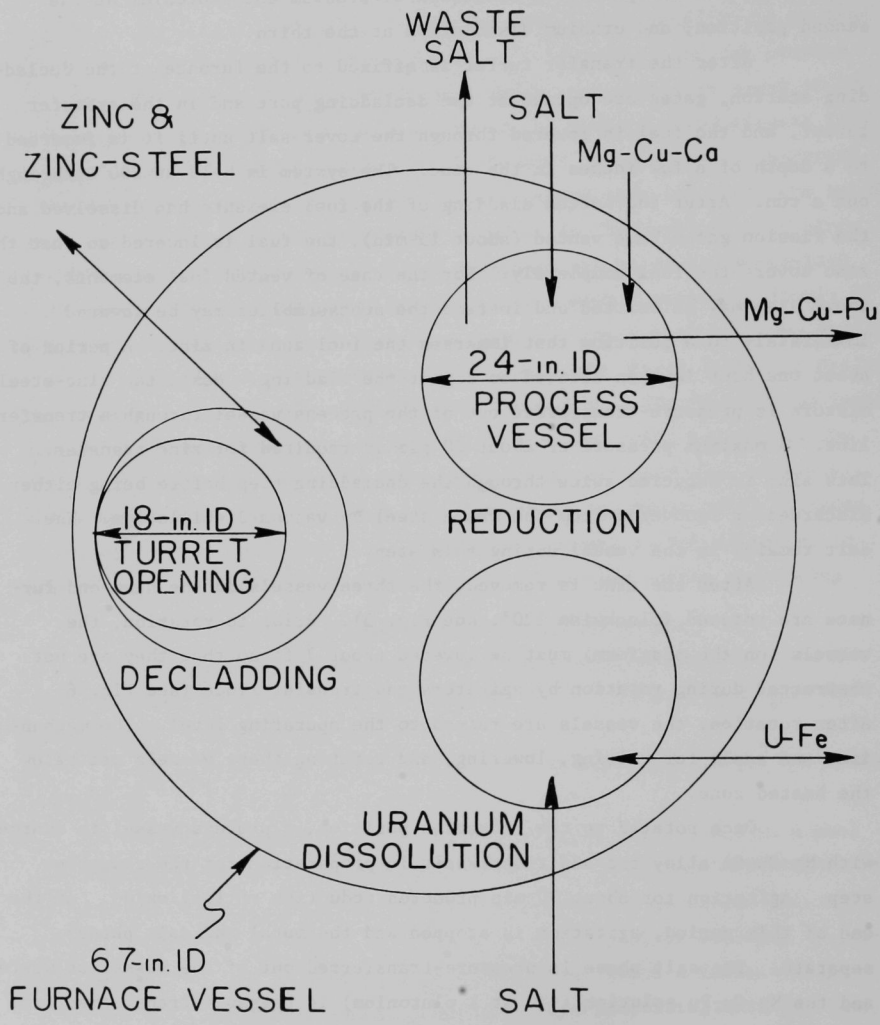

Figure 6

Head-End Processing Unit - Elevation View

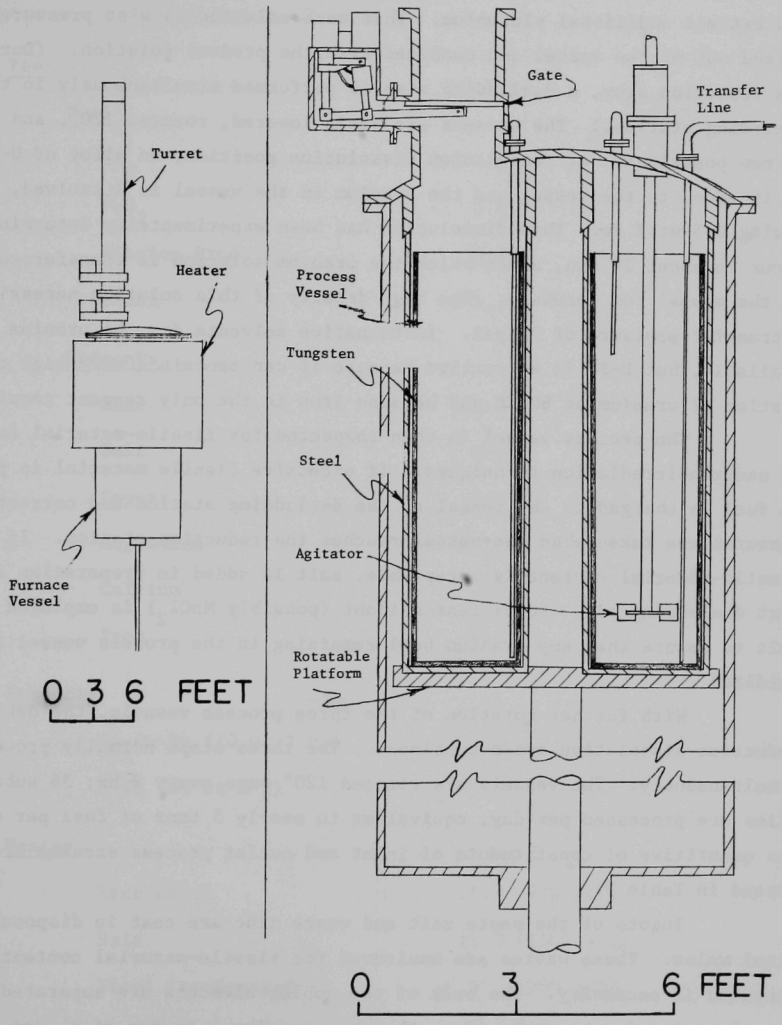

respectively, are required for the two transfers. The uranium remains as a precipitated phase in the bottom of the vessel. Next, a small amount of fresh Mg-Cu alloy is charged to the vessel to wash the precipitated uranium and extract additional plutonium. This wash solution is also pressure-transferred out of the vessel and combined with the product solution. (During the reduction step, a decladding step is performed simultaneously in the preceding station.) The vessels are again lowered, rotated 120°, and raised to new positions. At the uranium dissolution position, an alloy of U-12 wt % Fe is added to the vessel and the uranium in the vessel is dissolved, producing U-5 wt % Fe. This dissolution has been experimentally determined to occur in about 10 min, after which the uranium solution is transferred out of the vessel for recovery. The high density of this solution necessitates a transfer pressure of 75 psi. (Alternative solvents for the uranium are available, but U-Fe is attractive because it can contain a very high concentration of uranium at 800°C and because iron is the only reagent required.)

The process vessel is then inspected for fissile-material content by neutron-irradiation techniques. If excessive fissile material is present, no fuel is charged to the vessel at the decladding station and corrective measures are taken when the vessel reaches the reduction station. If the fissile-material content is acceptable, salt is added in preparation for the next decladding run. Sufficient oxidant (possibly $MnCl_2$) is employed in this salt to assure that any uranium heel remaining in the process vessel is oxidized.

With further rotation of the three process vessels, the decladding-reduction-dissolution cycle continues. The three steps normally proceed simultaneously. The vessels are rotated 120° once every 2 hr; 36 subassemblies are processed per day, equivalent to nearly 5 tons of fuel per day. The quantities of constituents of inlet and outlet process streams are listed in Table 2.

Ingots of the waste salt and waste zinc are cast in disposable steel molds. These wastes are monitored for fissile-material content and recycled if necessary. The bulk of the nobler elements are separated from the plutonium in the waste zinc, thereby removing a source of sludge in the

Table 2

Inlet and Outlet Process Streams

Basis: one operating day

(Quantities in tons except where noted otherwise)

Feed	
Fuel	
UO_2	4.17
PuO_2	0.44
Fission Products	0.19
Steel	6.7
Reagents	
Zinc	15.5
Salt	9.0
Copper	2.4
Magnesium	1.2
Calcium	1.5
Iron	0.2
Products	
Mg-Cu-Pu (10 wt % Pu)	3.9
U-Fe (95 wt % U)	3.8
Wastes	
Zinc-Steel	18.3 (750 gal)
Salt	11.3 (1500 gal)
Steel (compressed)	5 (200 gal)
Gas	16 ft^3 at 225 psi

acid dissolution step.

Dissolution of the Mg-Cu-Pu ingot in the acid dissolution step of a solvent extraction process would consume approximately 4.7 times as much acid as would be required for dissolution of an equivalent amount of UO_2-PuO_2 fuel. If U-Fe alloy is dissolved in addition to Mg-Cu-Pu, the total acid consumption would be about 5.9 times that for an equivalent amount of UO_2-PuO_2. The cost of the greater acid consumption is insignificant ($\sim$0.0008 mill/kW-hr), but the effects on dissolver design, gas handling, and waste disposal might be important. The effects on the suceeding process steps of adding magnesium, copper, and iron cations must also be evaluated. Dissolution kinetics have been demonstrated to be very good; the absence of iodine and tritium and of nobler metals (particularly ruthenium) from the plutonium dissolver is an obvious advantage.

A reducing solution of Mg-Zn-Ca is an attractive alternative to the Mg-Cu-Ca system. For this alternative, the resultant Mg-Zn-Pu solution could be concentrated by evaporating off the zinc and magnesium prior to acid dissolution. The Mg-Cu-Ca system is used in this design because its effectiveness as a reducing agent for sintered oxide fuel has been demonstrated during development of the Salt Transport Process (it was selected for the latter process because of its extraction characteristics in the pyrochemical step that follows reduction).

a. Fission-gas Containment

The cover gas in the processing vessel during decladding is composed of xenon, argon, and krypton. It is not maintained at a specific composition but is the mixture that results from the gases that enter the decladder, i.e., its composition depends on the type of fuel being processed and its fission-gas content. Since the input of argon to the decladder is low, the fission gases are collected in highly concentrated form. For the reference fuel, the composition is about 64% Xe, 29% Ar, and 7% Kr. The major addition of argon occurs when the transfer turrets are evacuated (after fuel decladding) and refilled with gas from the cell gas system; if the turret were not refilled with cell gas, cell contamination with radioactive gases would occur during discharge of the upper portion of the

subassembly from the turret and during charging of the next load of subassemblies to the turret.

The gas used to make pressure transfers of solutions between vessels is compressed to 100 psi and stored for reuse. Accumulated gases are removed periodically and further compressed to 225 psi for permanent storage in cylinders.

2. Zinc Decladding-Voloxidation Alternative

In this process alternative, zinc decladding would be followed by transport of fuel oxides to a voloxidizer unit in perforated refractory metal baskets. (In a rotary kiln voloxidation unit being developed at ORNL,[3] UO_2 is oxidized to U_3O_8 to effect evolution and removal of ^{131}I and the noble gases prior to acid dissolution.) Adequate ^{131}I removals have never been demonstrated using voloxidation,[1] and this process step may not be technically feasible. The following plant concept illustrates a zinc decladding facility (without reduction) that delivers declad fuel to the voloxidizer step of the aqueous process.

Subassemblies are taken in groups of three to the decladding vessel and lowered into one of four ports on the vessel, as described in detail below:

1. Three cropped subassemblies in the storage pool (Fig. 7) are assembled on a rack by the manipulator in the pool. The rack is conveyed under a partition into the transfer lock.
2. A steel turret (Fig. 8) for transporting fuel subassemblies is picked up from the turret storage rack by the large crane and is moved with the aid of a second crane through a sliding door into the transfer lock containing the three selected subassemblies. Each turret is about 1 1/2 ft in diameter and 15 ft high. Inside a turret are mechanisms for lifting and lowering a basket and fuel, as well as connections for forced argon cooling of subassemblies.
3. The turret is positioned over the rack containing the cropped subassemblies. The gate at the bottom of the turret is opened, and the engaging tool in the turret is lowered and

Figure 7

Plan View, 2nd Level, Conceptual Decladding Building

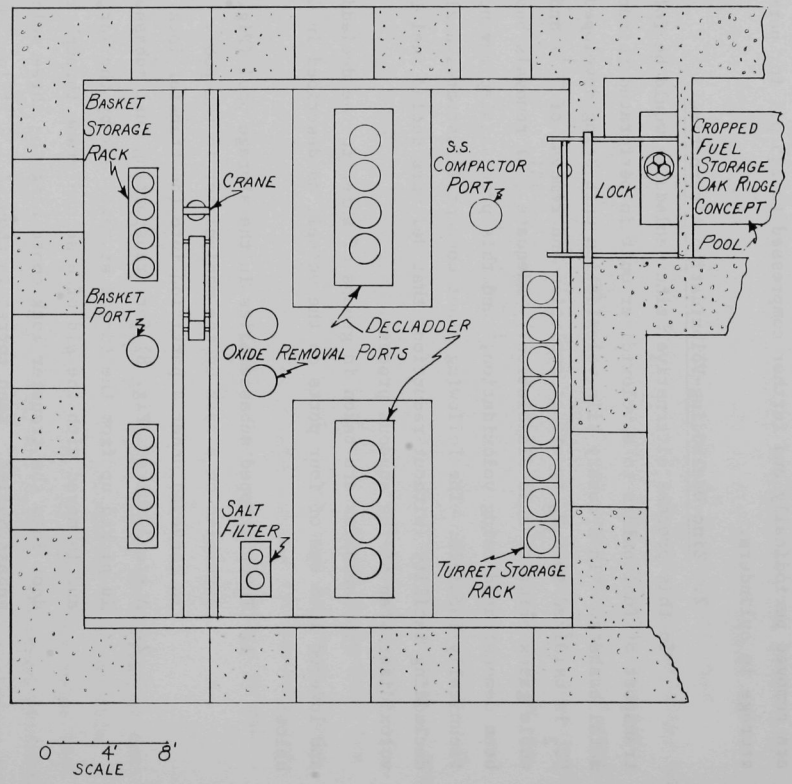

Figure 8

Conceptual Turret Design

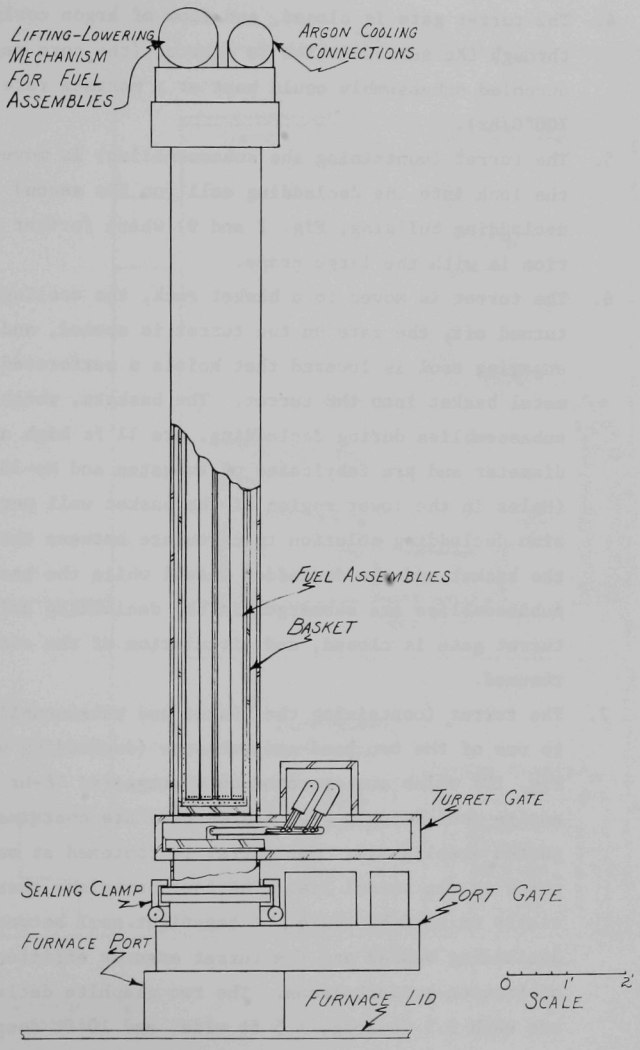

engages the subassemblies, which are hoisted into the turret. Sodium is allowed to drain from subassembly surfaces into the pool.

4. The turret gate is closed, and flow of argon cooling gas through the subassemblies is started (the core region of an uncooled subassembly could heat at a maximum rate of 700°C/hr).
5. The turret (containing the subassemblies) is moved out of the lock into the decladding cell (on the second level of the decladding building, Fig. 7 and 9) where further manipulation is with the large crane.
6. The turret is moved to a basket rack, the cooling gas is turned off, the gate on the turret is opened, and a basket engaging tool is lowered that hoists a perforated refractory metal basket into the turret. The baskets, which contain the subassemblies during decladding, are 11 ft high and 16 in. in diameter and are fabricated of tungsten and Mo-30 wt % W. (Holes in the lower region of the basket wall permit the zinc decladding solution to circulate between the inside of the basket and the decladder vessel while the basket and subassemblies are submerged in the decladding solution.) The turret gate is closed, and circulation of the cooling gas is resumed.
7. The turret (containing the basket and subassemblies) is moved to one of the two head-end furnaces (decladding vessels, Fig. 10) which are operated on a staggered 48-hr cycle. An entire decladding vessel and furnace are contained in a supported steel shell. The turret is fastened at one of four ports in the vessel lid. The four ports are charged sequentially on an 8-hr cycle. A gas-tight seal between the decladding vessel and the turret ensures efficient retention of fission-product gases. The two graphite decladding vessels are each 9.5 ft long, 1.5 ft wide, and 10 ft deep (inside

Figure 9

Elevation View, Conceptual Decladding Building

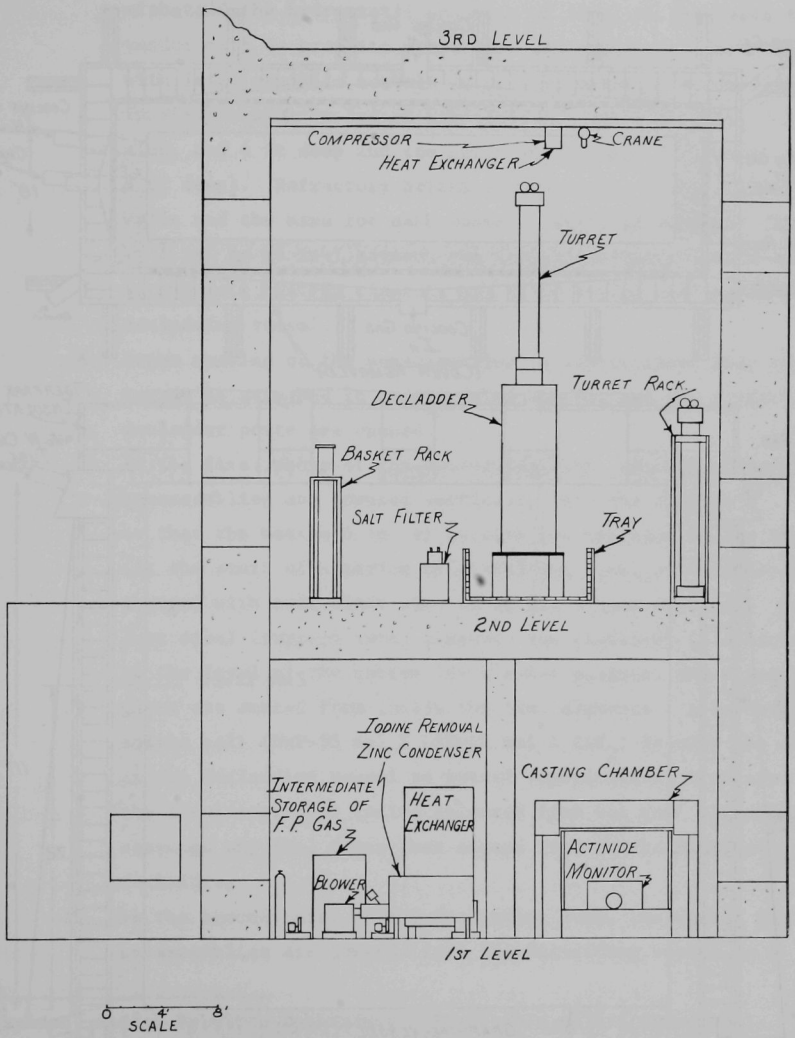

Figure 10

Conceptual Decladding Vessel

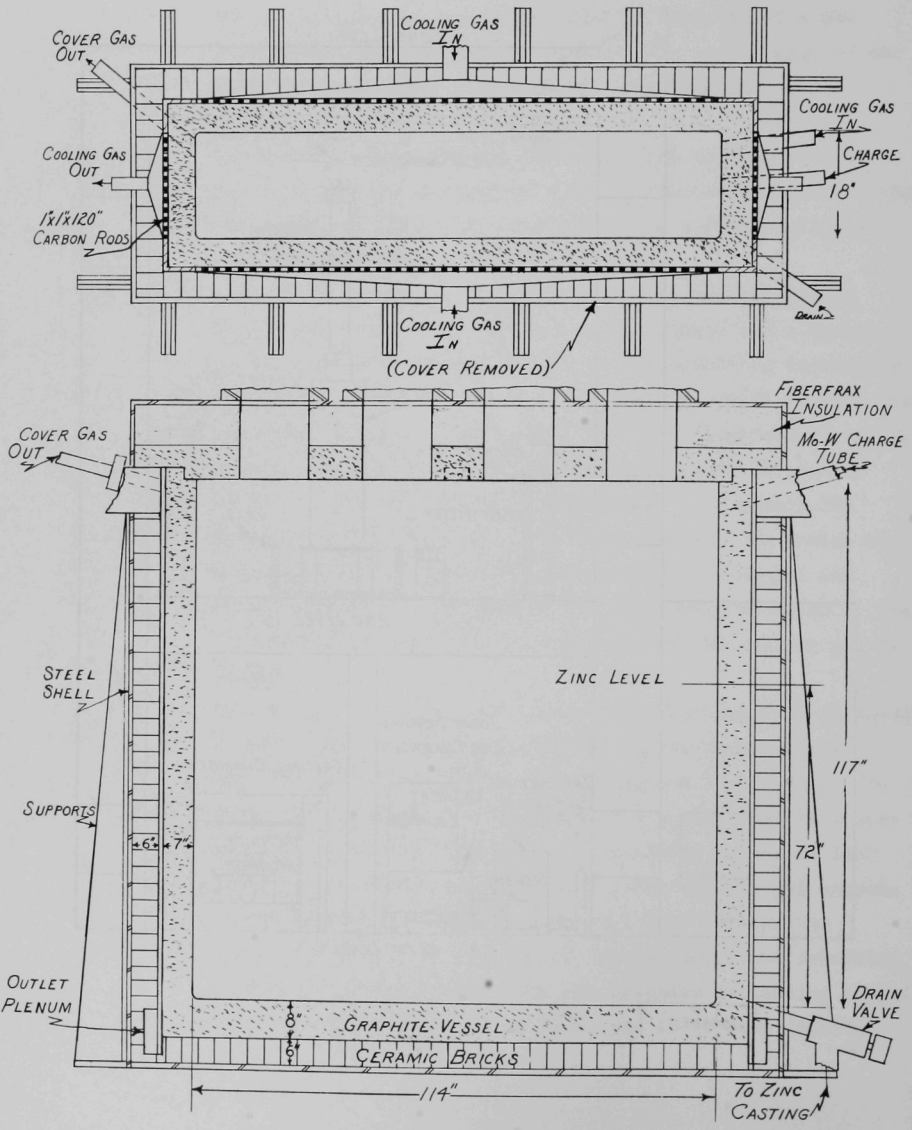

dimensions). This size was selected on the basis of achieving a 15 wt % loading of stainless steel in zinc. The corners are rounded to minimize stresses. A wall thickness of 7 in. and a base thickness of 8 in. were selected as sufficient to withstand the hydrostatic pressure of zinc, on the basis of vendor data on graphite properties and industrial experience with large graphite vessels (e.g., two sizes of molds used in steel-making by Amsted Laboratory,[10] one 6 ft long, 2 ft wide, and 4 ft deep and the other 18 ft long, 2 ft wide, and 6 ft deep). Refractory bricks provide 6-in.-thick insulating walls and the base for each vessel. Vertical channels (1 in. by 1 in. by 96 in.) between the insulation and graphite walls accommodate heating elements and allow forced cooling of the decladding vessel.

8. Argon cooling of the subassemblies is discontinued when the turret is attached to a decladding vessel, and the turret and decladder ports are opened.
9. In the first phase of the decladding step, the basket and subassemblies are lowered vertically into the zinc melt so that the bottom 4 in. of pellets are immersed in the zinc. (At the start of a series of decladding runs, a decladder is charged with sufficient zinc to declad 5 tons of fuel.) Stainless steel (support bars, sleeves, and cladding) is dissolved to the level of the bottom few blanket pellets, and fission gases are vented from inside the fuel elements. A layer of molten salt (NaF-55 mol % LiF-10 mol % CaF_2) is over the zinc in the decladding vessel to retard vaporization, trap some of the fission-product iodine released from the fuel elements, and scavenge any fuel fines that escape from the basket during decladding.
10. In the second phase of the decladding step, the basket and subassemblies are lowered into the decladding vessel to a

---

[10] Carlson, Amsted Research Laboratory, Blusenville, Ill., personal communication to N. M. Levitz, ANL (1969).

depth of 72 in. in zinc to dissolve the remaining stainless steel cladding and sleeve surrounding the blanket and core oxide. The UO_2-PuO_2 is retained within the basket. As a criticality safeguard, only the quantity of oxide from three subassemblies is allowed in a basket.

11. During decladding, the cover gas leaving the decladder is piped through a zinc condenser, a heat exchanger, and fission-gas compressors and is permanently stored in cylinders in fission gas storage facilities.
12. The top 5 ft of the stainless steel subassembly (which has remained above the zinc level) and the basket containing the UO_2-PuO_2 are raised into the turret. Zinc-stainless steel is allowed to drain from the basket into the decladding vessel. The turret and decladder ports are closed, and radioactive gases between the gates are pumped to the decladder cover-gas system, after which the space between the gates is filled with cell gas. During gas pumpout, the temperature at the center of the fuel in the basket rises at a maximum rate of about 800°C/hr, and if the transport operations are interrupted at this stage for about an hour, some fuel starts to melt. However, even at steady state, only the center of the oxide mass would be molten, and the highest temperature anywhere on the turret wall would be 800°C, an acceptable temperature.
13. The turret and its contents are moved to the fuel oxide dumper with no forced cooling. The turret gate is opened, and the pellet-laden basket is lowered into the dumper and disengaged from the turret.
14. The turret gate is closed, and the turret is evacuated to the decladder cover-gas system and filled with cell gas.
15. The undissolved top sections of the subassemblies contained in the turret are transported to the waste-metal discharge port, lowered into the decontamination cell, and disengaged

from the turret. The top sections of the subassemblies are probably decontaminated with acid. The empty turret is returned to the subassembly loading area.

16. In the fuel oxide dumper, the basket walls are raised, and the fuel oxide is pushed with a hoe-shaped pusher from the basket into a hopper for subsequent feeding to the voloxidizer.
17. The basket is hoisted out of the fuel oxide dumper and moved to an inspection and cleanup area.
18. After inspection of the basket and removal of any significant quantities of fuel, the basket is stored in a rack.
19. Decontaminated top sections and cropped ends of subassemblies are compacted to steel cubes in a press for subsequent burial as waste.
20. After one day's processing (about 5 tons of fuel), decladding operations are switched to the second head-end furnace. Cleaning of the decladder that has been used during the previous 24-hr processing starts with insertion of an agitator into the decladder to mix the zinc-stainless steel mixture and the cover salt. This causes fuel oxide particles to collect in the salt phase. The decladding vessel is normally kept at ~800°C for all process operations to avoid time-consuming heating and cooling cycles.
21. After a period of agitation, most of the salt is transferred out of the decladder and circulated through a filter to remove suspended fuel and other insolubles; the filtered salt is later recycled to the decladder. Before the salt is eventually discarded by casting as waste ingots, monitoring is done and any significant quantity of plutonium is removed.
22. The bottom valve of the decladder is opened, and zinc-iron slurry is drained into a heated graphite melt distributor

(modeled after industrial practice)[11-13] for the casting of 32 ingots (10-in. dia by 6-ft long) in steel molds lined with Fiberfrax (see Fig. 11).

23. The decladder valve is closed, and the decladder is cleaned and inspected.
24. Fresh zinc may be added to the decladder through a heated Mo-W tube from the zinc-premelt vessel. Alternatively, zinc-stainless steel drained from decladding vessels may be filtered to remove insoluble stainless steel constituents and recycled to the decladder.
25. Waste zinc-steel ingots are cooled and monitored for plutonium (e.g., with a neutron generator and an instrument for detecting high-energy fission gamma rays). Any sections of waste ingot thought to contain plutonium may be cut out for reprocessing.
26. Waste zinc-steel ingots are sealed in their steel molds, which serve as permanent containers.

On the basis of material and heat balances around the decladding vessel and preliminary process-cell layouts, an inert-gas process cell, approximately cube-shaped and 30 ft on a side, would be adequate. The cell would include a floor-port fuel unloading station; a saw for trimming excess hardware from the fuel subassemblies; two decladding vessels; turret-storage racks; salt-storage tanks; scales, hoists, and manipulators; and a number of auxiliary components.

---

[11] K. J. Brondyke and F. F. McCormick, Aluminum, Fabrication and Forming, Vol. III, K. R. Van Horn, Ed., American Society for Metals, Metals Park, Ohio (1967), pp. 41-42.

[12] W. H. Dennis, Extractive Metallurgy, Sir Isaac Pitman & Sons, Ltd., London (1965), pp. 327-344.

[13] D. R. Cliffe, Technical Metallurgy, Edward Arnold Publishers, Ltd., London (1968), pp. 251-276.

Figure 11

Waste Zinc Casting Chamber

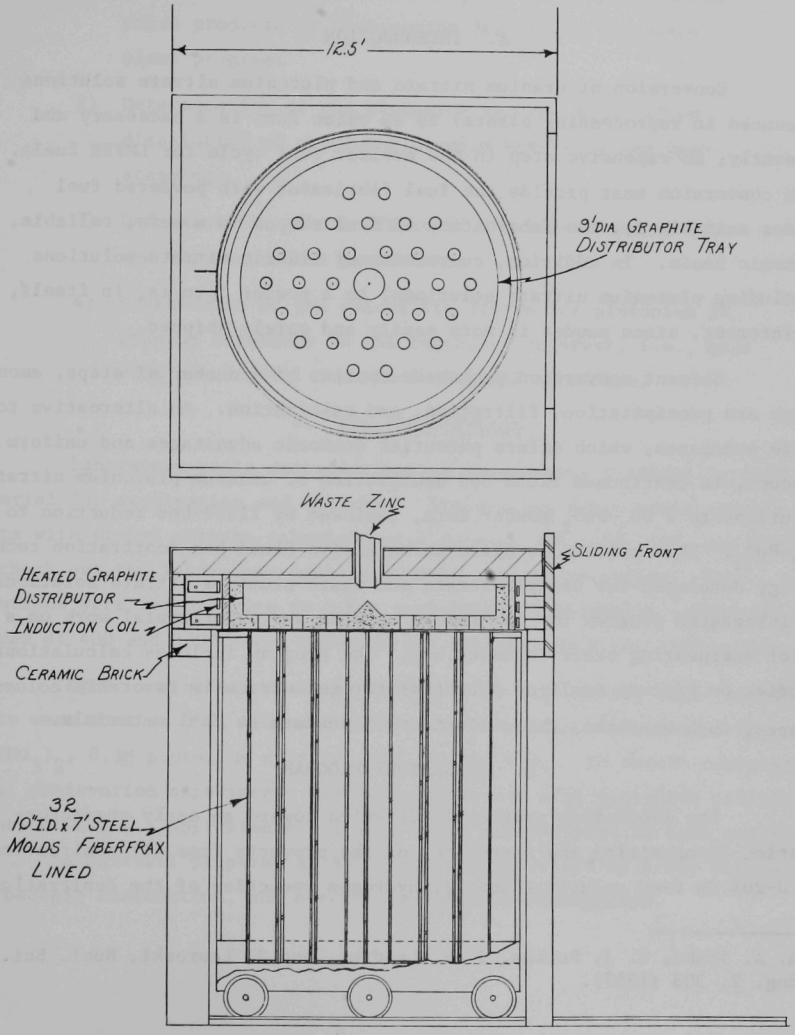

II. CONTINUOUS CONVERSION OF U/Pu NITRATES TO OXIDES

(N. M. Levitz, G. J. Vogel, S. Vogler, F. G. Teats, and R. V. Kinzler)

A. INTRODUCTION

Conversion of uranium nitrate and plutonium nitrate solutions (produced in reprocessing plants) to an oxide form is a necessary and presently, an expensive step in the nuclear fuel cycle for LMFBR fuels. This conversion must provide the fuel fabricator with powdered fuel oxides suitable for the fabrication of fuel shapes on a safe, reliable, economic basis. In addition, conversion of fissile nitrate solutions (including plutonium nitrate solutions) to a powder form is, in itself, of interest, since powder is more easily and safely shipped.

Current conversion processes consist of a number of steps, among which are precipitation, filtration, and calcination. An alternative to these processes, which offers potential economic advantages and uniform product, is continuous fluid-bed denitration of uranium-plutonium nitrate solutions to a UO_3-PuO_2 powder form, followed by fluid-bed reduction to UO_2-PuO_2. This process is based on extensive fluid-bed denitration technology developed for uranyl nitrate and waste aluminum nitrate solutions.[1] An integrated program for laboratory studies and experimental work on a pilot engineering scale is described. The program includes calculational studies on process scale-up potential for geometrically favorable column shapes, such as slabs, and evaluation of powders as fuel materials.

B. LABORATORY PROGRAM

The laboratory program is directed toward an early characterization (composition and structure) of the products from (1) denitration of U-20% Pu feed solutions and (2) hydrogen reduction of the denitration

---

[1] A. A. Jonke, E. J. Petkus, J. W. Loeding, and S. Lawroski, Nucl. Sci. Eng. 2, 303 (1957).

product. Other subjects under study or under consideration include the following:

1) Development of a dissolution procedure for the mixed oxide products of denitration for use in the pilot-plant program.

2) Determination of the plutonium valence state after dissolution of uranium-plutonium materials and upon standing.

3) Determination of the effect of plutonium valence (IV and VI) on product properties.

4) Measurement of the solubility limits for plutonium in uranium solutions in the region of interest, i.e., near 2.0M total metal ions including 20% plutonium.

1. Drop-Denitration

Laboratory-scale drop-denitration experiments provided initial material for examination and analysis. Preliminary denitration experiments with uranyl nitrate solutions were done at 300, 400, 500, and 600°C to check out the laboratory-scale equipment and the procedure. The solutions were fed dropwise to a hot surface for denitration. Products formed at 400 and 500°C were selected for analysis by X-ray diffraction.

After installation of the equipment in a glovebox, three experiments were done at 300, 450, and 600°C with solutions containing 1.2M $UO_2(NO_3)_2$, 0.3M plutonium nitrate, and 2 to 4M HNO_3. To obtain comparative data, denitration experiments were also performed with plutonium nitrate solutions alone. Approximately 6 g of oxide was prepared in each experiment. The material prepared at 450°C was characterized by X-ray diffraction, microscopic examination, and electron-microprobe examination.

a. X-ray Diffraction Examination of Denitration Products

X-ray diffraction examinaton of the product of the denitration of uranyl nitrate at 500°C showed the product to be gamma-UO_3, whereas the product formed at 400°C consisted of gamma-UO_3 and $UO_3 \cdot H_2O$. The examination of the mixed oxide product indicated the major phase to be gamma-UO_3; PuO_2 was reported as a possible minor phase, although only a limited number of characteristic lines were observed. For the oxide derived from denitration of plutonium nitrate solutions at 450 and 300°C, PuO_2 was the only phase found. The crystallinity of the powder was poor, with the 450°C oxide being more crystalline than the 300°C oxide. The poor crystallinity resulted in diffuse diffraction lines which made calculation of lattice parameters difficult.

b. Electron-Microprobe Examination

A sample of the oxide powder prepared at 450°C was introduced into a metallographic mount suitable for electron-microprobe examination. The material was polished, the final polish being with Linde A (alumina abrasive, 0.3-μm diameter). After polishing, a 50Å coating of gold was sputtered on the sample surface to prevent contamination of the equipment.

To examine the sample, the electron beam (0.5 μm in diameter), was focussed initially upon a spot in one of the product particles. The characteristic X-rays emitted by the plutonium and the uranium were counted simultaneously (always for a fixed period of time) using separate detectors. This single-point counting procedure was repeated randomly across the area of the particle. The counting rates were corrected for background, and the uranium-to-plutonium count ratios were calculated. The constancy of this value is a measure of the microscopic homogeneity of the powder particles. The count ratios of uranium to plutonium for two particles, summarized in Table 1, show considerable scatter, but no spots that were free of plutonium were found.

The first product was reexamined using the same electron beam

Table 1

Uranium and Plutonium Distribution in Oxide Particles Prepared by Denitration at 450°C

	U/Pu Count Ratio			
	Particle 1 0.5-μm-dia spot	Particle 2 0.5-μm-dia spot	Particle 1 8 x 10-μm area	Particle 1 80 x 100-μm area
	6.34	7.28	5.11	5.14
	6.87	7.96	3.44	5.35
	4.31	6.82	6.89	4.72
	7.18	6.71	7.81	4.55
	7.30	7.11	8.02	5.01
	3.94	5.76	4.68	5.56
	6.24	3.95	5.58	
	7.14	5.30	4.23	
	2.11	6.21	6.41	
	2.27		6.69	
	6.32		4.89	
	6.65		3.83	
	8.75		3.33	
	7.83		6.50	
	5.10		5.36	
	11.3			
	4.80			
Mean	6.14	6.34	5.52	5.06
S.D.	±2.28	±1.20	±1.50	±0.38

and the same time interval. However, instead of focusing on a single spot, the electron beam systematically swept an 8 by 10 μm area, with several such counts being made in different areas of the particle. In yet another counting procedure, data were obtained while the electron beam scanned an 80 by 100 μm area of the first product particle. The data from these area scans were treated in the same manner as the single-point data.

The results obtained by scanning a large area (80 by 100 μm) indicate that the overall homogeneity is good, the standard deviation being only about ±7.5%. However, scans by point counting and by scanning an area 8 by 10 μm did indicate localized differences in concentration. No attempt has been made yet to compare these data with FFTF specifications.

For reference, a standard UO_2-PuO_2 sintered pellet with a uranium-to-plutonium weight ratio of 3.89 gave a uranium-to-plutonium count ratio of 5.94 when examined by single-point counting. The pellet and denitrated oxide powders are not strictly comparable since the matrix of the standard was UO_2 and the matrix of the denitrated powders was UO_3. It should be emphasized that the purpose of the electron-microprobe study was to determine the homogeneity of the powder and not to determine the actinide content.

c. Autoradiography

With this technique the ionization produced in a cellulose nitrate film by plutonium alpha radiation from UO_3-PuO_2 is used to measure the homogeneity of plutonium distribution. The molecular structure of the cellulose nitrate is deformed by ionization when energy is transferred from the alpha particles. When the cellulose nitrate film is subsequently placed in a sodium hydroxide solution, the deteriorated area is attacked and removed, leaving cone-shaped voids which form an image.

The procedure for preparing an autoradiograph was as follows: The UO_3-PuO_2 powder to be examined was mixed with a plastic that sets

at room temperature to form a casting 1 in. in diameter. When the casting had hardened, it was polished in the same manner as the specimen for electron-microprobe examination. After polishing, the casting was wrapped in 1-mil Mylar to prevent plutonium contamination. A cellulose nitrate sheet (~1 in. square) was placed on the surface of the casting, with only a single thickness of Mylar between the powder and the cellulose nitrate film. The cellulose nitrate was exposed to the alpha radiation for 1 min. while a heavy weight on the cellulose nitrate provided close contact of the cellulose nitrate and powder. After the exposure, the cellulose nitrate was placed in 6.25M NaOH at 50°C for 4 min., and then was washed with distilled water. After air-drying, the cellulose nitrate was examined microscopically. Preliminary results with this technique have indicated that the plutonium distribution in the powder is rather uniform. These results confirm the data obtained by electron-microprobe examination.

2. Dissolution of Oxide Produced by Denitration

Dissolution in nitric acid of UO_3-20 wt % PuO_2 powder produced in laboratory experiments by drop-denitration was investigated. This step will allow recycling the denitration product from the pilot plant into uranium and plutonium nitrate solutions for further denitration and will thus minimize the plutonium inventory in the glovebox. Dissolution experiments of a scoping nature were performed on a gram scale with U-20% Pu oxide produced by drop-denitration at 300°C. Since the rate of dissolution of the PuO_2 fraction is known to be limiting, the plutonium content of the solution was monitored (by liquid scintillation counting) as a function of time. About 95% of the oxide was dissolved by stirring for 2 hr in concentrated HNO_3 (16M) at 95°C to yield a solution approximately 0.35M in heavy metal.

Additional dissolution experiments were performed on mixed oxides produced by drop-denitration at 300, 450, and 600°C. The experimental conditions included the following: nitric acid molarity, 5 to 16;

dissolution temperature, 95 to 120°C; and final actinide concentrations of 0.35 and 1.5M. Data indicated (1) that oxide prepared at higher temperatures was more difficult to dissolve, (2) that the rate of oxide dissolution was not affected significantly by the dissolution temperatures, (3) that the dissolution rate was not affected by a higher final actinide concentration, when dissolution was with 16M nitric acid, and (4) that the fraction of plutonium dissolved is greater at the higher acid concentration.

Laboratory-scale experiments were also performed to compare the rate of dissolution in concentrated nitric acid of PuO_2 prepared at 300°C with the rate of dissolution of the plutonium in UO_3-20 wt % PuO_2 prepared at the same temperature. The experimental conditions were 16 molar nitric acid, 120°C dissolution temperature, and actinide molarities in the final solutions of 0.35 and 1.5. Data indicated that plutonium in the UO_3-PuO_2 material dissolved more rapidly than pure plutonium oxide (~99% as compared with 30-50% in 5 hr). Nevertheless, recycling of plutonium oxide in the pilot plant facility may be possible by redissolving the oxide and allowing a heel to remain in the dissolution vessel.

A tentative procedure for pilot-plant use has been proposed for dissolving UO_3-PuO_2 in nitric acid. This procedure takes advantage of the ready dissolution of the UO_3 fraction. This fraction would be dissolved in 3M nitric acid and transferred to a reservoir. The PuO_2 heel would be dissolved in two steps: a portion of the plutonium would be dissolved by agitation with 10M nitric acid at 90°C and the solution transferred to the reservoir; then a similar step would be performed to dissolve the remainder of the PuO_2 heel with 16M nitric acid. Any undissolved material, which should be small in amount, would remain as a heel in the dissolution vessel.

A laboratory experiment (experiment 10) was carried out to test the feasibility of this procedure. Initially, a 2.95 g sample of UO_3 -20 wt % PuO_2 (prepared at 450°C) was mixed with 8 ml of 3M nitric acid for 1 hr at room temperature. After the residue settled, the supernatant

solution was decanted. Then approximately 8 ml of 16M HNO_3 was added to the residue and dissolution was continued at 95°C with stirring. Samples of the new supernatant solution were taken after 1/2, 2, and 5 hr of stirring. For material balance purposes, after 5 hr of dissolution, the new supernatant was decanted and the residue was dissolved in 16M nitric acid containing 0.05M HF.

All of the samples taken during the dissolution experiment (experiment 10) were analyzed for plutonium by liquid scintillation counting. The results are summarized in Table 2.

Table 2

Dissolution of UO_3-PuO_2

(Oxide prepared by denitration at 450°C)

Operation	Time (hr)	Experiment 10[a] Pu Dissolved (%)	Experiment 10[a] Cumulative Pu Dissolved(%)	Experiment 1[b] Cumulative Pu Dissolved
UO_3 Dissolution	1	14	14	
PuO_2 Dissolution	1/2	45	59	78
	2	29	88	81
	5	11	89	98
Residue Dissolution		11		2

[a] The conditions of the dissolution are given in the text.

[b] The oxide was dissolved directly in 16M nitric acid at 95°C.

Approximately 14% of the plutonium in the mixed oxide dissolved in the 3M nitric acid. In the second part of the test, after 1/2 hr at 95°C, 59% of the plutonium had dissolved; after 2 hr, 88% had dissolved; and after 5 hr, 89% had dissolved. For comparison purposes in Table 2,

results are included from an experiment (experiment 1) in which the same mixed oxide was dissolved directly in 16M nitric acid at 95°C. This experiment was included in those discussed in the first paragraph of this section. The results of experiment 10 agree reasonably well with the results of the direct dissolution experiment 1.

Samples were also submitted for X-ray fluorescence analysis to establish the disposition of the uranium. Results indicated that about 70% of the uranium dissolved in the 3M nitric acid and about 30% dissolved in the 16M nitric acid. Application of heat to the 3M nitric acid dissolution should improve the uranium dissolution rate.

C. ENGINEERING PROGRAM

A fluid-bed denitration pilot plant has been constructed to convert uranium nitrate and plutonium nitrate solutions and mixtures of these solutions to oxides. Because of the broad experience with cylindrical columns in earlier denitration work,[1] initial investigations will be done with a stainless steel cylindrical fluid-bed denitrator 4-in. in diameter, which is considered critically safe for feeds containing up to 20% plutonium. A parallel effort will be the development of a slab-shaped column, which offers nuclear criticality advantages upon scale-up of high-plutonium systems. A 4-in.-dia Lucite fluid-bed column (representing a mockup of the denitrator) was constructed to evaluate features of the denitrator design.

In the initial experiments, uranium solutions will be denitrated to prove the reliability of the equipment and instrumentation systems and to identify those operating variables that are significant to the control of the particle size of the powder in the fluid bed. Then, work with U/Pu solutions will begin.

1. The Denitration Process

In a fluid-bed denitration process, a heated bed of uranium oxide (typical of the denitration product) is fluidized with air. A solution of

uranyl nitrate is sprayed into the bed. The liquid droplets either wet the particles and thermally decompose to deposit a fresh oxide layer, or decompose in the gas phase to form solid particles. An overflow arrangement keeps the bed inventory in the denitrator constant.

Uranyl nitrate hexahydrate (UNH) is decomposed thermally according to the following reaction:

$$UO_2(NO_3)_2 \cdot 6H_2O \xrightarrow{\text{heat}} UO_3 + 1.86\ NO_2 + 0.14\ NO + 0.57\ O_2 + 6H_2O$$

The exact composition of the gaseous products is uncertain and varies with the temperature of denitration. The reaction is endothermic, absorbing about 260,000 Btu/lb-mol uranium at 230°C.[1] More heat than for UNH is required for decomposition of our solutions, which typically are more dilute than UNH and contain excess nitric acid. Usual denitration temperatures range from 275 to 400°C.

2. Equipment

A simplified drawing of equipment for the denitration experiments is presented in Figure 1. The equipment consists of a fluidizing-gas preheater, a fluid-bed denitrator, nitrate solution preparation and metering tanks, secondary filter, condenser, demister, heater, and HEPA (High Efficiency Particulate Air) filter. Instrumentation consists of appropriate temperature and pressure sensors with local or panelboard readouts, controllers, recorders, and a data logger. The major process items are installed in an existing 3- by 4-module glovebox.

The fluid-bed denitrator consists of three separately flanged parts--the cone-shaped gas-distributor section, the denitration section, and the filter chambers.

The denitration section is fabricated of 4-in.-dia schedule 40 type 304 stainless steel pipe, 32 in. long. A spray nozzle and temperature or pressure sensors can be positioned at 3-, 6-, or 9-in. levels. The

Figure 1

Equipment Components of 4-in.-Dia Denitration Pilot Plant

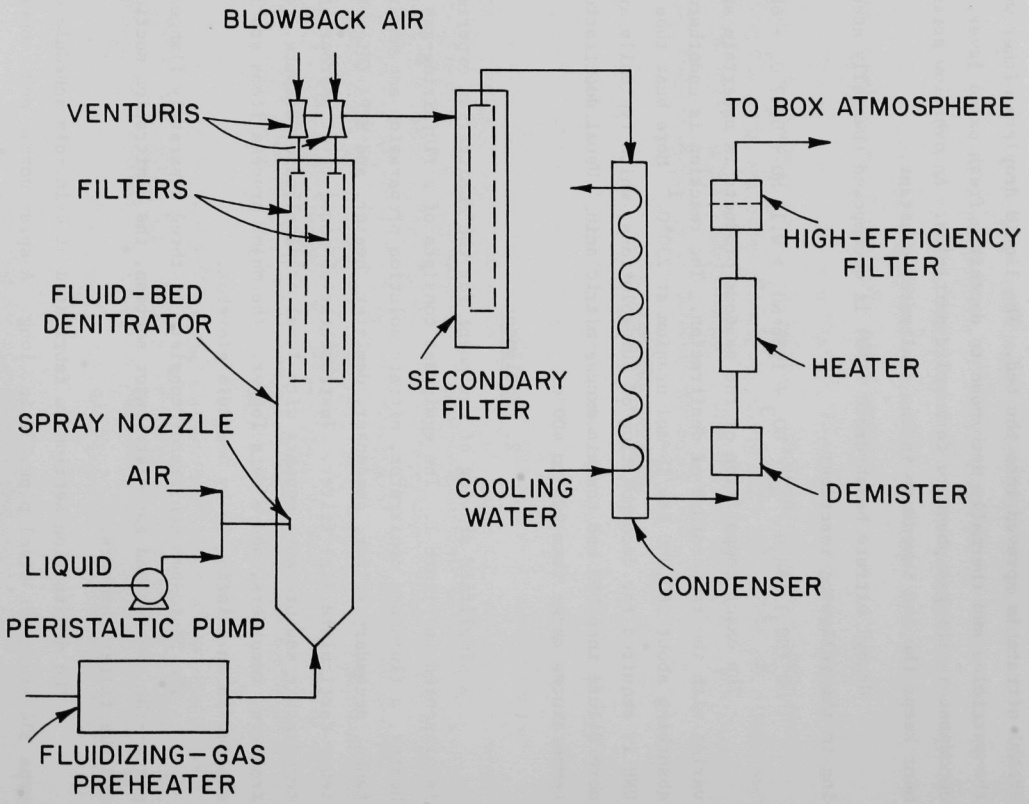

denitration section is heated by twelve 2000-W Watlow[2] resistance heaters, copper-spray-bonded to the exterior wall. The heaters are electrically wired in groups of three; each group's heat input is adjusted by a Variac.[3] Two of the Variac circuits include West temperature controllers.

The filter chamber is fabricated of 4-in.-dia schedule 40, type 304 stainless steel pipe and is 47 in. long. Installed in it are two sintered stainless steel filters.[4] The filters are 18 in. long, and have a nominal 10-μm pore size. The filters can be blown back manually or automatically by a timer preset for blowback duration and frequency. During a run, the two filters would be blown back alternately. Blowback air at 100 psig from the laboratory supply is stored in a 400-psi-rated stainless steel cylinder. The filter chamber is kept at less than 200°C during a denitration run.

The condenser is of impervious graphite,[5] and is 6 in. in diameter. The gases enter at the top and leave at the bottom, as shown in Figure 1. The condenser is cooled by chilled (35-40°F) water. Recycled coolant water is, in turn, cooled by a 3-ton refrigeration unit. The condensate from the condenser is collected in a 9-gal stainless steel (300 series) tank equipped with a sight glass and a bottom drain. Advantages of condensing (rather than scrubbing with caustic or sorbing on a solid) in this experimental setup are (1) the acid can be used to dissolve product urania-plutonia, thus allowing recycle of this material to the denitrator, (2) fewer liquid transfers out of and into the alpha box will be required, and (3) condensation appears to be simpler and cheaper than the other two methods.

---

[2] Product of Watlow Electrical Co., St. Louis, Missouri.

[3] Product of General Radio Co., West Concord, Massachusetts.

[4] Product of Pall Trinity Micro Corporation, Cortland, New York.

[5] Product of Carbone Corporation, Boonton, New Jersey.

The instrument panel[6] from an earlier facility is being used with slight modification for the denitration pilot plant. Included is an automatic data logger. Data generated during a denitration run will be fed into an IBM 360 System via a Remote Access Data Station (RADS), and a readable output (graphs and tables) will be produced.

The merits of batchwise and continuous preparation of nitrate feed solution were compared. Batch preparation, in which the entire batch is prepared before a run, has the following advantages:

1) The overall run time is shorter.

2) The solution composition is known (by analysis) and remains uniform.

3) An operator's time and attention are not diverted during a run to make the feed solution.

4) The equipment is simpler.

5) Fewer analytical samples are required.

Advantages of the continuous preparation method, in which oxide and nitric acid would be added continuously to a 1-hr supply in the feed tank, are as follows:

1) A denitration run may be continued indefinitely.

2) The inventory of plutonium can be smaller than for the batch method.

3) The size of feed tanks is about two-thirds that for batch preparation.

---

[6] G. J. Vogel, E. L. Carls, and W. J. Mecham, "Engineering Development of Fluid-Bed Fluoride Volatility Processes. Part 5. Description of Pilot-scale Facility for Uranium Dioxide - Plutonium Dioxide Processing Studies," USAEC Report ANL-6901, Fig. 17, p. 59 (1964).

Batch preparation is presently considered the more practical procedure for our experiments.

3. Mockup Tests

Tests were performed in a plastic mockup of the denitrator to determine the capability of differential pressure indicators to detect filter rupture, partial plugging, or plugging at gas flow rates up to 9 cfm (∿1.5 ft/sec). Results indicated that these types of malfunction would be detected.

Other tests were performed to determine if a shift in particle-size distribution in the bed (as a result of particle growth or fines production) could be detected from continuously recorded pressure-drop data for the fluid bed. Three alumina mixtures were tested--one with a balanced particle-size distribution, one with 40% fine (<200 mesh) particles, and one with 40% coarse (>40 mesh) particles. The frequency of the pen trace (the zig-zag motion) remained fairly constant, whereas the amplitude of the trace was slightly larger for the coarse mixture than for the fine. Additional data will be required before conclusions can be drawn regarding the use of Δp data to monitor particle-size distribution.

As a result of other mockup column work with inert alumina beds, the design of the product withdrawal pipe on the pilot-plant denitrator was changed: For product takeoff, a pipe extending vertically through the bed was initially considered, but because of the possibility that liquid nitrate feed would be sprayed onto the pipe and dry, causing solids to build up, an alternative design was tested in which the overflow pipe was fitted flush with the denitrator wall. Although with this design (the overflow pipe was installed in one of the six ports available on the denitrator wall), the pipe is not at a steep angle with the horizontal (which would promote solids flow), tests indicated that solids could be withdrawn satisfactorily through the pipe.

4. Criticality Considerations

A preliminary criticality analysis of the pilot-plant system indicates that boron-containing glass Raschig rings would allow the use of a feed storage vessel with a relatively large diameter (12-in.-diameter). Such fixed nuclear poisons have been in use for about 10 yr at other nuclear sites.

In related work to determine whether an increase in the quantity of PuO_2 in a process vessel could be measured with external instrumentation, experiments were made with ~1/2 to 1 kg of UO_2-1.78 wt % PuO_2 and UO_2-20 wt % PuO_2 powder (shielded with 1/4-in. stainless steel to simulate the effect of a vessel wall). A scintillation-type counter fitted with a gamma probe was found to be promising for this application. Additional experiments may be made later with larger quantities of plutonium.

III. IN-LINE ANALYSIS IN FUEL FABRICATION

(J. G. Schnizlein, M. J. Steindler)

A. INTRODUCTION

The cost of fuel fabrication represents a major portion of the total fuel-cycle costs for power reactors, and reduction of such costs is necessary to improve the competitive economic position of power-producing nuclear reactors. The cost of the fuel cycle for fast breeder reactors (FBR) is currently estimated to be about 2 mills/kW-hr. Of this, 0.8 mill/kW-hr is fabrication cost.[1] It is expected that improved technology will decrease fuel-cycle costs to a level considerably below that for boiling-water reactors and pressurized-water reactors (about 1.75 mills/kW-hr).

Because of the rigor of the FBR fuel specifications, analytical methods and their application to the fabrication process and to the product have assumed great importance in the economics of the fuel cycle. It is important to develop analytical methods capable of determining the physical and chemical properties of the fuel with the precision and accuracy required by the relationship between fuel performance and properties. Large-capacity fabrication plants will require automated and perhaps continuous in-line analytical methods.

B. FUEL PROPERTIES

The absence of experimental data relating the effects of various fuel properties to fuel performance required rigorous specifications for ceramic fuels. Of the ceramic fuels being considered, uranium-plutonium oxides are the most developed and consequently may be expected to be the fuel in the first commercial FBR. The specifications and required precision for Fast Flux Test Facility (FFTF) fuel are presented in Table 1.

---

[1] "Liquid Metal Fast Breeder Reactor (LMFBR) Program Plan," Vol. 8. Fuel Recycle, USAEC Report WASH-1108, p. 28 (1968).

Table 1

FFTF Specifications:

Fuel Composition, Physical Properties, and Fuel Impurities

	UO_2 Powder	PuO_2 Powder	Mixed Oxide or Pellets	Method	Precision
Composition					
U Content	0.5 to 5-mg sample >87.6% U	<2000 ppm		Coulometry	0.2%
Pu Content	--	>87% Pu		X-ray Fluor.	0.5%
Pu/M	--	--	20.00% 24.00%		±0.40 (2% rel.) ±0.48 (2% rel.) Core zone avg. ±0.1 0.5%
Isotopic Content	^{235}U = 0.71 ± 0.05%	239+241 = 88.0 ± 0.5% 241 Max. 2.5% 238 Max. 0.15% 240 Balance	Same	Mass Spec.	
O/M	2.04-2.10	--	--		±0.03 (1.5% rel.)
	--	1.95-2.00	--		±0.025(1.25% rel.)
	--	--	1.97		±0.02 (1% rel.)
Property					
Density (% of Theor.)[a]	94% for 0.8-mm (+20 mesh) particles after specified sintering procedure	90% for 0.8-mm (+20 mesh) particles after specified sintering procedure (cont'd)	93%		±2%(±0.01 g/cc) 2%

Table 1 (Cont'd.)

FFTF Specifications:

Fuel Composition, Physical Properties, and Fuel Impurities

Property (Continued)	UO_2 Powder	PuO_2 Powder	Mixed Oxide or Pellets	Method	Precision
Homogeneity			0.2-g sample 20.0±0.5% PuO_2 24.0±0.6% PuO_2 95% single phase		
Particle Size	thru 325 mesh (44μm) 50% 20μm 95% 30μm Max 100μm	thru 325 mesh (44μm) 50% 20μm 95% 30μm Max 100μm[b]	Max 100μm[b] for pellet grains		
Impurity					
H_2O	0.4%	0.4%	30 ppm	Dry at 200°C, followed by electrolysis of H_2O swept into electrolytic cell	±5 ppm
Gases other than H_2O			0.15 cc(STP) / 3-g sample	Vacuum outgas	±7%
Total impurities, ppm	3000	3000	3000	Spectrographic	
Σ Cu,Zn,Si, Ti, ppm	800	800 (cont'd)	800	Spectrographic	

Table 1 (Cont'd)

FFTF Specifications

Fuel Composition, Physical Properties, and Fuel Impurities

	UO_2 Powder	PuO_2 Powder	Mixed Oxide or Pellets	Method	Precision
Impurity (Cont'd.)					
Σ Ag,Mn,Mo,Pb, Sn, ppm	200	200	200	Spectrographic	
Carbon, ppm	150	200	150	Combustion	
Fluoride, ppm	25	25	25	Pyrohydrolysis	
Chloride, ppm	10	25	25	Pyrohydrolysis	
Sulfate, ppm	1000	1000	1000		
Nitrogen, ppm	200	200	200	Fusion-Kjeldahl	

[a] Theoretical densities are calculated on the basis of UO_2 density of 10.965 g/cc and PuO_2 density of 11.46 g/cc.

[b] In BNWL-1090, maximum particle size was relaxed from 50 to 100μm if confidence limit verifies that 300μm is the upper limit and agglomeration is infrequent.

Further correlations between performance and initial fuel properties are required. Results of irradiation experiments have not been consistently related to initial fuel properties even though such results are used to define overall performance and fuel changes due to high burnup. These new correlations should clarify how adequate performance is related to the principal properties of the fuel materials, as well as the degree of analytical precision required during fabrication. Important properties include (1) U/Pu ratio, (2) density, (3) homogeneity, (4) oxygen-to-metal ratio, (5) thermal properties (melting point, thermal expansion, and thermal conductivity), and (6) chemical purity. The specifications, precision and methods of measurement of these properties are discussed below to provide insight to choices of potential in-line analytical methods.

1. U/Pu Ratio

Determination of the U/Pu ratio of fuel will be part of any conceivable fabrication procedure. Plutonium concentrations being considered for various FBR fuels range from 8 through 30%. The more probable contents appear to be 15, 18, 20, and 25%. Ternary phase diagram studies by Markin and Street[2] indicate that oxide material in the substoichiometric O/M region and containing up to 40% Pu is single phase at room temperature and above.

Controlled-potential coulometry is the method currently recommended for determining plutonium and uranium content of mixed-oxide fuel.[3] An alternative technique for determining the U/Pu ratio may be in-line X-ray fluorescence. X-ray fluorescence analysis is a sensitive, nondestructive method: exciting radiation (from an X-ray tube or a radioactive source) impinges on the sample and causes the emission of radiation that

---

[2] T. L. Markin and R. S. Street, J. Inorg. Nucl. Chem. 29, 2265-2280 (1967).

[3] "LMFBR/FFTF Fuel Development Analytical Chemistry Program," USAEC Report LA-4407 (1970).

is characteristic of the elements present in the sample; by this method, uranium and plutonium concentrations can be determined rapidly and accurately.

2. Density

The density specification for pellets containing 24% Pu is 93±2% of theoretical density (i.e., 10.31±0.22 g/cc). Pellet densities in the range of 93 to 95% of theoretical appear to be achievable. Pellet densities are calculated from the average lengths and average diameters of weighed pellets. Pellets are loaded into cladding tubes with an annular gap of 2 to 8 mils, resulting in smear densities ranging from 80 to 88%. Precise characterization of pellet precursor material is essential in order to attain the prescribed pellet density. Sintering tests are required and the density of particles greater than 20 mesh is measured to a precision of 0.01 g/cc by mercury displacement.

3. Homogeneity

Homogeneity refers to the uniform distribution of plutonium in samples of individual pellets. The specified acceptance criterion for homogeneity, in addition to a specification for particle sizes of make-up powders, is that a 0.2-g sample of mixed oxide be within 0.5 or 0.6% of the prescribed plutonium content (see Table 1). There is an indication that if plutonium-containing particles are too large, an undesirable positive Doppler coefficient is obtained in the reactor. The initial specification of 50 μm as the maximum particle diameter for mixed-oxide fuel was revised[4,5] to 100 μm.

---

[4] E. R. Astley, "Fast Flux Test Facility Quarterly Technical Report, March-May, 1969," USAEC Report BNWL-1090 (July 1969).

[5] See Trans. Am. Nucl. Soc. 12(2), 703 (1969) where the influence of PuO_2 particle diameter on fuel temperature during transients is discussed.

4. Oxygen-to-Metal Ratio

In determining oxygen-to-metal (O/M) ratio for samples between 2 and 100 mg, a thermogravimetric method[6] of analyzing for oxygen is specified. The O/M specifications are 2.07 ± 0.03 for UO_x and 1.975 ± 0.025 for PuO_x powder. The O/M value of 1.97 ± 0.02 for mixed-oxide or coprecipitated oxide pellets is attained in the sintering process.

The initial ratio of O/M in the charged fuel affects both thermal conductivity and the compatability of fuel with cladding during irradiation. The probable desired range of values for the O/M ratio is 1.95 to 1.99. Since the O/M ratio changes during irradiation due to the thermal gradient and the oxidation of fission product metals (i.e., Mo, Ba, Sr, Zr, and Nb) in the fuel, additional study may be required before a value of O/M for fuel fabrication can be set.

A method for the determination of the O/M ratio that may be adaptable for in-line use will be tested. This method depends upon the measurement of lattice parameters of the fuel material by X-ray diffraction techniques.

5. Thermal Properties

Melting point, thermal expansion, and thermal conductivity are the thermal properties of principal interest. These are dependent on the Pu/U ratio, O/M ratio, and density of the fuel.

6. Chemical Purity

Impurity contents of 1500-3000 ppm iron or silicon have been stated to be deleterious; however, more recent results may show them to be beneficial by ensuring that oxide fuel remains substoichiometric, thereby minimizing the corrosion of cladding. Moisture as an impurity has caused

---

[6] W. L. Lyon, "Oxygen-to-Metal Ratio in Solid Solutions in UO_2 and PuO_2," USAEC Report GEAP-4271 (1963).

excessive gas pressure, as well as cladding corrosion that led to cladding failure.

Although little effort has been made at this time to provide in-line analytical techniques for determining impurity levels, the general problem will be looked at in detail later.

C. RESULTS

In order to lower the cost of fabrication of large quantities of fuel material for the FBR program, automated analytical methods should be developed that furnish adequate characterization of essential fuel properties. For operation of large-capacity fabrication plants on a sound economic basis, continuous in-line analytical methods for process control and product analysis are desirable. The accuracy and precision of such analytical methods will affect the fraction of acceptable material produced and thus influence the overall cost of the fabricated fuel. In cases where it may not be possible or desirable to use continuous in-line procedures for all analyses, more economical or more convenient discontinuous methods will be considered.

1. U/Pu Ratio in Fuel

Determination of the U/Pu ratio by in-line X-ray fluorescence spectrometry appears to be feasible for both pellets and powder. However, greater efficiency and sensitivity than routinely available is required to attain the precision of 0.5%. Methods for accomplishing improvements of the technique are discussed below.

Liebhafsky[7] has calculated the loss of intensity, at each of nine identified processes, for a flat-crystal spectrograph fluorescence apparatus. The three greatest loss factors of X-rays are in the following

---

[7] H. A. Liebhafsky, X-ray Absorption and Emission in Analytical Chemistry, John Wiley & Sons, New York, 1960, p. 27.

processes:

1. Efficiency of X-ray production (1Å), 3.7×10^{-3}.
2. Fraction absorbed and re-emitted by the sample, 4.4×10^{-6}.
3. Fraction emerging from collimator (geometric factor), 1.6×10^{-5}.

Techniques for improving the efficiency of these processes are discussed below.

In X-ray generation with existing equipment, adequate data apparently will be obtained at a maximum of 2.5 kVA, using a tungsten-target X-ray fluorescent tube at 40-60 kV peak and appropriate milliampere ratings. The use of isotope sources for excitation is not being considered at present because their intensities are considerably lower than the more conventional tubes.

The fraction absorbed and re-emitted, the largest loss factor, has been the subject of considerable research in recent years. Absorption includes scattering from surfaces, voids, and crystallites, as well as the absorption accountable in terms of mass absorption coefficients of other elements present. When the characteristic radiation from one element has enough energy to excite the characteristic radiation of another element in the sample, enhancement or secondary fluorescence may take place. This occurs in uranium-plutonium oxides because PuLα excites ULα. In thorium-uranium oxides ULα excites ThLα.

Quantitative analysis by a fluorescence technique normally requires a set of standards covering the range of variables of interest, such as composition (element concentration and matrix content), density, crystallite size, and absorption coefficients. Criss and Birks[8,9] have formulated methods (utilizing modern computers) whereby X-ray fluorescence can be

---

[8] L. S. Birks, X-ray Spectrochemical Analysis, Chem. Analysis, Vol. 11, Interscience Publ. (1969).

[9] J. W. Criss and L. S. Birks, Anal. Chem., 40, 1080 (1968).

calculated from fundamental parameters. Calculation should greatly decrease the number of standards necessary. The program, originally run on a CDC-3800, has been obtained at ANL and will be tried on the IBM-360 system.

The theory and experimental effects of inhomogeneities in samples have been reviewed by Berry.[10] To simplify the relationships, relative intensities are taken as linearly dependent on packing fractions and exponentially dependent on differences of linear absorption coefficients and particle size.

Experiments will be performed in an attempt to improve the count rate (factor 3 above) by the use of collimators with wider slits. For a particular collimator, it must be verified that the two peaks are resolved adequately and that the background count has not increased sufficiently to interfere with the precision of counting. The use of nondispersive detectors (e.g., GeLi) also would improve factor 3, lowering this loss to one-hundredth or less of its present values, but the available resolution (250 eV at low count rates) is not sufficient to resolve the ULα and PuLα lines at high intensities.

a. Experimental

To demonstrate the feasibility of using X-ray fluorescence spectrometry directly on $(U\text{-}Pu)O_2$, experiments were performed with ThO_2-UO_2 mixtures. Because of the identical atomic number relationship, results for Th-U should be similar to results for U-Pu without the problems of plutonium hazards. Powdered mixtures were prepared containing 10, 20, 30, and 40% UO_2 in ThO_2 and were examined with the X-ray spectrograph. Data have been obtained for eight power levels of the X-ray generator and two sizes of masks covering the sample. These data make possible the presentation of relative intensity values (Table 2 and Fig. 1). Consistent with expecta-

[10] P. F. Berry, T. Furuta, and J. R. Rhodes, Particle Size Effects in Radioisotope X-ray Spectrometry, Advances in X-ray Analysis, Vol. 12, Plenum Press, 1969, pp. 612-632.

Table 2

Relative Spectrometric Intensities for ThO_2-UO_2 Mixtures

Sample	1/2-in. Mask		1/4-in. Mask		Relative I/I_{MO_2}			
					UO_2		ThO_2	
	U(c/sec)	Th(c/sec)	U(c/sec)	Th(c/sec)	1/2-in.	1/4-in.	1/2-in.	1/4-in.
UO_2	10304	--	2765	--	1.0	1.0	0	0
40 UO_2-60 ThO_2	3584	8960	960	2419	0.348	0.347	0.773	0.762
30 UO_2-70 ThO_2	2688	9600	720	2624	0.261	0.260	0.829	0.827
20 UO_2-80 ThO_2	1856	10304	499	2861	0.180	0.180	0.889	0.901
10 UO_2-90 ThO_2	832	10624	230	2842	0.081	0.083	0.917	0.895
ThO_2	--	11584	--	3174	0	0	1.0	1.0

Figure 1

X-Ray Fluorescence: ThO_2-UO_2

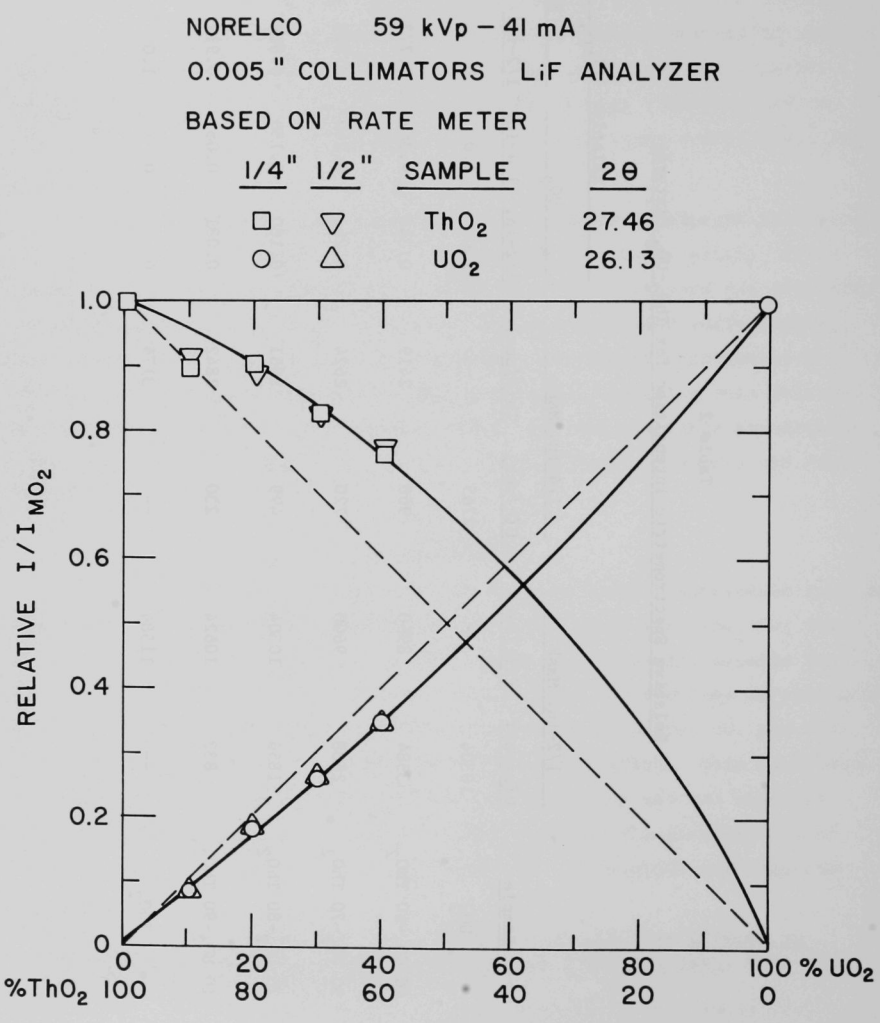

tions, matrix effects of absorption are shown for uranium and enhancement effects for thorium. Consideration of the fluorescence spectra and absorption edges of Th, U, and Pu suggests some enhancement (Ref. 8, pp. 71-75) of thorium emission by uranium fluorescence but less enhancement of uranium emission by plutonium.

It is generally accepted that the precision of X-ray fluorescence analysis is limited by counting statistics. For the requirements of 0.5% precision at the 95% confidence level, careful attention to statistics will be required in this program. Plummer[11] has derived a relationship for counting statistics based on a desired precision and confidence level. Using his relationship for two peaks and one background, the optimum total counting time (based on preliminary 20% UO_2-80% ThO_2 data) may be as much as 1200 sec. Changing the collimators to provide greater count rates should reduce the counting time required to achieve the desired precision, provided that the background rate is not increased too much.

2. Oxygen Content of Fuel

The O/M ratio of fuel material (UO_2-PuO_2) may be one of the more important factors controlling the changes in fuel during irradiation. The O/M ratio presently specified for the FFTF driver-fuel pellets is 1.97 ± 0.02. The recommended FFTF analytical method is based on the weight change of a sample upon heating. Heating the sample to 800°C in a He-6% H_2 gas stream saturated with H_2O at 0°C is claimed[12] to produce an O/M = 2.000. Measurements are claimed to be reproducible to 0.001 O/M units, but the accuracy of the method is not known due to a lack of standards.

---

[11] L. N. Plummer, Counting Strategy in X-ray Emission Spectroscopy, Appl. Spect. 23, 583 (1969).

[12] "Analytical Chemistry Methods in Support of Driver Fuel Fabrication," USAEC Report BNWL-1024 (1968).

Markin, Walter, and Bones[13] have reviewed the various methods of O/M determination applied to O/U, O/Pu, and O/(U + Pu). These authors described a method using the reduction of hyperstoichiometric oxide with CO at 850°C and compared the results with those from a high-temperature galvanic cell, polarographic determination of U(VI), and oxidation to U_3O_8. (Hypostoichiometric mixed oxide was first oxidized with oxygen to $(U,Pu)O_{2+x}$ and then reduced with CO.) The claimed accuracy of the CO method is ±0.001 O/M for hyperstoichiometric oxide and ±0.002 O/M for the two-stage process (including preliminary oxidation) required for hypostoichiometric oxide.

The methods currently relied on for acceptable precision and accuracy are slow and destructive. A method based on physical properties such as the lattice parameter could be made rapid and nondestructive and might be adaptable for in-line use. The basis for such a method is outlined below, although some reservations of its applicability would need to be dispelled by experimental work.

Extensive studies of the U-Pu-O ternary system by X-ray diffraction have been performed at Harwell[2, 13-17] and Karlsruhe.[18] When the O/M ratio is carefully controlled at 2.00, Vegard's relationship between UO_2 and PuO_2 has been demonstrated, i.e., a linear change of lattice cell size with a change of plutonium content.

---

13 T. L. Marken, A. J. Walter, and R. J. Bones, "The Determination of Oxygen/Metal Ratios for Uranium, Plutonium and (U,Pu) Oxides," Report AERE-R-4608 (1964).

14 N. H. Brett and A. C. Fox, J. Inorg. Nucl. Chem. 28, 1191-1203 (1966).

15 E. R. Gardner, T. L. Markin, and R. S. Street, J. Inorg. Nucl. Chem. 27, 541-551 (1965).

16 G. Dean, Proceedings 3rd Int. Conf. on Plutonium, London, 1965, pp. 806-827.

17 T. L. Markin and E. J. McIver, Proceedings 3rd Int. Conf. on Plutonium, London, 1965, pp. 845-857.

18 H. M. Mattys, Actinide Rev. 1, 165-182 (1968).

It is generally accepted that deviations in oxygen stoichiometry are accompanied by an effective change of valence of either the uranium or plutonium, respectively, in the hyper- and hypostoichiometric regions.[2,9] The addition of oxygen oxidizes uranium toward a valence of five and the removal of oxygen reduces plutonium toward a valence of three.

In the hyperstoichiometric region, Brett and Fox[14] have demonstrated a linear relationship for the lattice parameter between PuO_2 and hypothetical "U_2O_5" for the cubic phase in equilibrium with orthorhombic (U_3O_8-type) phase. Markin and Street[2] contend that the theoretical Vegard plot should be drawn with respect to U_4O_9. However, lattice parameters of 5.4285Å and 5.4275Å for $(Pu_{.11}U_{.89})O_{2.34}$ and $(Pu_{.15}U_{.85})O_{2.30}$, respectively, appear to support the relationship with "U_2O_5". Lynds and others[19] demonstrated for the uranium oxides that two relationships are involved. UO_{2+x} and U_4O_{9-y} are two different entities; UO_{2+x} has interstitial oxygen, whereas U_4O_{9-y} is a defect structure. The relationships to lattice parameter are:

$$UO_{2+x}: \quad a_o = 5.4705 - 0.094x \quad (0 < x < 0.125)$$

$$U_4O_{9-y}: \quad a_o = 5.4423 + 0.029y \quad (0 < y < 0.31)$$

It seems reasonable that a similar relationship between the lattice parameter and O/M should exist in the ternary system.

In the hypostoichiometric region, Gardner et al.[15] have determined, by high-temperature X-ray diffraction, the lattice parameter for the body-centered cubic phase PuO_{2-x} which is in equilibrium with the face-centered Pu_2O_3, stable above 600°C, and has an O/M ratio greater than 1.61.

---

[19] L. Lynds et al., Advances in Chem. Series--Non-Stoichiometric Compounds, Vol. 39, p. 59 (1963).

Although PuO_{2-x} is commonly indexed as body-centered cubic, the lattice parameter for the related face-centered structure is one-half that for bcc. Markin and Street[2] have proposed a phase diagram for the ternary Pu-U-O system and have determined some lattice parameters for various plutonium (III) contents. Their lattice parameter data support a linear relationship for the lattice parameter between UO_2 and "$PuO_{1.5}$". Some modifications have been proposed by Karlsruhe,[18] but they do not affect the hypostoichiometric, single-phase region between 8 and 30% Pu which is of interest for FBR fuel.

Data have been located in the literature relating the lattice parameter to O/M ratio for ternary materials between 10 and 40% Pu (for which adequate analyses for Pu and O_2 can be presumed). The data for 15, 18, 20, 25, 30, and 42% Pu are presented in Fig. 2. The data from Markin and Street[2] for 42% Pu cover the largest range of O/M and indicate that the slope is 0.0047Å per 0.02 O/M ratio (the FFTF specification). The data of Gibby[20] for 25% Pu indicate a slope of 0.0060Å per 0.02 O/M ratio. The data of Schmitz[21] for 18% Pu indicate a significantly different slope but were measured over a limited range. No line was drawn through the earlier data of Baily and Lyon[22] for 20% Pu because of the limited range of O/M ratios and the inclusion of a point with an oxygen content greater than 2.00.

---

[20] R. L. Gibby, "The Effect of Oxygen Stoichiometry on the Thermal Diffusivity and Conductivity of $U_{0.75}Pu_{0.25}O_{2-x}$," USAEC Report BNWL-927 (1969).

[21] F. Schmitz, "Structures and Properties of $(U,Pu)O_2$ Containing Non-Active Fission Products. A Simulation of Irradiated Nuclear Fuel," Report CEA-R-3795 (1969).

[22] W. E. Baily and W. L. Lyon, "Electrical Properties of Pu-U Mixed Oxide System," USAEC Report GEAP-4675 (1965).

Figure 2

Lattice Parameter for U-Pu Oxides as a Function of O/M Ratio

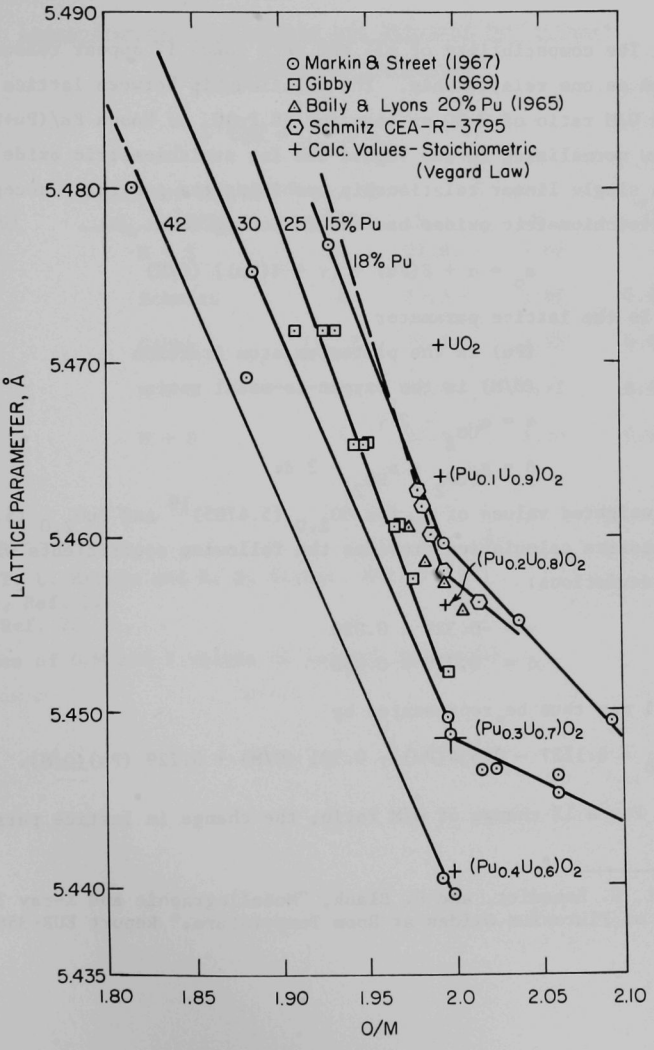

Each set of data was subjected to a least squares fit of the relation $O/M = C-Da_o$ where a_o is the lattice parameter. The values of the coefficients, C and D, and the standard deviations are presented in Table 3.

The compatibility of all the data makes it appear reasonable to treat them as one relationship. The relationship between lattice parameter and O/M ratio of 2.00 or less for $(U,Pu)O_2$ of known Pu/(Pu+U) ratio will allow normalizing to the Vegard law for stoichiometric oxide (O/M = 2.00). A single linear relationship combining the generally accepted Vegard law for stoichiometric oxides has the following form:

$$a_o = \alpha + \beta(Pu) + [\gamma + \delta(Pu)]\ (O/M) \qquad (1)$$

where a_o is the lattice parameter

(Pu) is the plutonium atom fraction

(O/M) is the oxygen-to-metal ratio

$\alpha = a_{UO_2} - 2\gamma$

$\beta = a_{PuO_2} - a_{UO_2} - 2\delta.$

Imposing weighted values of a_o for $UO_{2.0}$ (5.4705)[19] and $PuO_{2.0}$ (5.3952),[23] a least squares calculation provides the following coefficients with their standard deviations:

$\gamma = -0.321 \pm 0.020$

$\delta = 0.229 \pm 0.058$

Equation 1 may thus be represented by

$$a_o = 6.1127 - 0.534(Pu) - 0.321\ (O/M) + 0.229\ (Pu)(O/M). \qquad (2)$$

For a 1% change of O/M ratio, the change in lattice parameter is

---

[23] C. Sari, U. Benedict, and H. Blank, "Metallographic and X-ray Investigation of Plutonium Oxides at Room Temperature," Report EUR-3564 (1967).

Table 3

Least-Squares Coefficients and Standard Deviations of O/M Ratios of U-Pu Oxides

$$O/M = C - D\, a_o$$

Pu/(U + Pu)	Source of O/M and a_o Values[a]	No. of Data	C	D	$\sigma_{O/M}$
0.15	M + S	2	22.0	3.66	--
0.18	Schmitz	4	17.8	2.89	0.0004
0.25	Gibby	14, 7[b]	22.5	3.75	0.008
0.30	M + S	4	24.4	4.12	0.002
0.42	M + S	4	25.5	4.33	0.003

[a] M + S; T. L. Markin and R. S. Street, Ref. 2.
Schmitz, Ref. 21
Gibby, Ref. 20.

[b] 14 values of O/M and 7 values of lattice parameter, a_o.

0.0055Å, which is easily measured since it is about ten times the usual precision of lattice-parameter measurements.

Figure 3 presents a relationship of lattice parameters to O/M ratio within the substoichiometric single-phase region bounded by Vegard relationships for UO_2-PuO_2 and UO_2-"$PuO_{1.5}$". The cross-hatch bands indicate the limits of the single-phase regions based on the phase diagram of Markin and Street.[2] Dashed lines represent values from the correlation and points represent interpolations from the experimental data presented in Figure 2.

Data collected by White[24] during fabrication of mixed oxides in three sintering atmospheres at 1650°C provided lattice parameters and O/M measurements obtained by a thermogravimetric method (oxidation-reduction) and a chemical method (fusion). The right-hand column of Table 4 presents O/M values obtained by translations of White's lattice parameters by means of Equation 2.

Consideration of the published literature and the above correlation of lattice parameter with O/M indicates that analysis of O/M within the desired precision is feasible by X-ray diffraction measurement of lattice parameters.

---

[24] C. D. White, ANL, private communication (October 1967).

Figure 3

Lattice Parameter for U-Pu Oxides as a Function of Plutonium Content

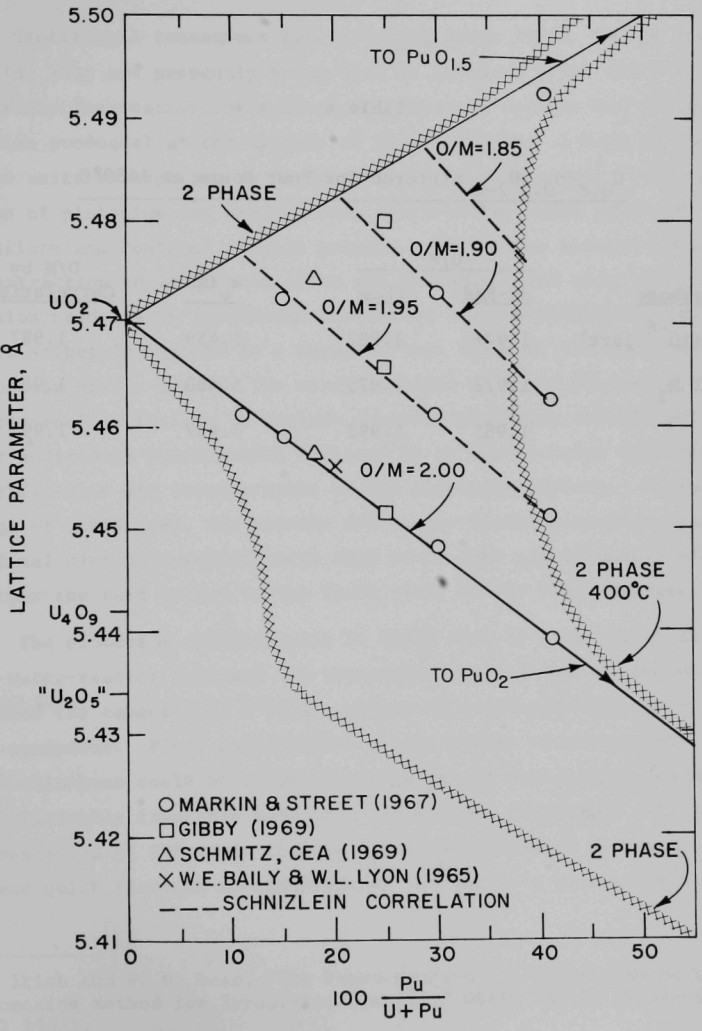

Table 4

$U_{0.8}Pu_{0.2}O_{2-x}$ Sintered for Four Hours at 1650°C

Atmosphere	O/M		a_o (Å)	O/M by Correlation
	Ox-Red	Chem		
Vac (10^{-6} Torr)	1.977	1.982	5.459	1.987
He-6% H_2	1.972	1.976	5.460	1.984
He	1.985	1.992	5.457	1.994

IV. ADAPTATION OF CENTRIFUGAL CONTACTORS IN LMFBR FUEL PROCESSING

(G. Bernstein, D. Grosvenor, J. Lenc, N. Quattropani)

A. INTRODUCTION

Centrifugal contactors with settling zones 10 in. in dia and about 13 in. long are presently being used at Savannah River (SRP) to process production-reactor fuels (i.e., to separate uranium and plutonium from fission products) at throughputs of 40-60 gal/min. A bank of these large size units is expected to be suitable for a Purex-type[1] first cycle extraction of plutonium and uranium from short-cooled LMFBR fuels if the feed is dilute and contains soluble poisons. (The Purex process employs solvent extraction to separate uranium and plutonium from each other and from fission products in irradiated uranium or uranium-plutonium fuel. The solvent is tributylphosphate in a kerosene-type diluent, and the aqueous phases contain nitric acid.) The usual practice in Purex processing of light-water-reactor fuel is to include a second plutonium solvent extraction cycle for additional purification followed by an ion-exchange treatment for final purification and concentration of the plutonium product. In the processing of LMFBR fuel, the streams fed to the second plutonium cycle and the final plutonium purification step would have significantly smaller volumes than the feed stream to the first cycle of the Purex process.

The plutonium concentration in LMFBR fuel is much higher than in light-water-reactor fuel and the throughput for a 5 metric tons/day plant would exceed the capacity of a single column of critically safe ion-exchange equipment. Final purification of the higher concentration plutonium solutions could be accomplished better in centrifugal contactors having a critically favorable geometry. Additional advantages that have been demonstrated at SRP would include minimized radiation damage to the solvent and quick flushout of equipment at the end of a processing campaign.

---

[1] E. R. Irish and W. H. Reas, "The Purex Process - A Solvent Extraction Reprocessing Method for Irradiated Uranium," USAEC Report HW-49483A (April 1957).

The plutonium nitrate product from this step is expected to be suitable for use as feed material for continuous conversion to oxide in a fluidized-bed denitration operation.

A program has been undertaken to extend the centrifugal contactor design developed at the Savannah River Laboratory of E. I. duPont de Nemours & Co.[2-7] to a configuration suitable for efficient handling of plutonium in the plutonium isolation steps during solvent-extraction processing of LMFBR fuels. The streams fed to the plutonium purification steps will have significantly smaller volumes than the feed stream to the first cycle of the process. It is therefore feasible to reduce the physical size of the contactor. The principal advantage sought is an increase in nuclear safety by limiting the diameter of the unit to a critically favorable dimension, while maintaining a relatively high capacity by increasing bowl length and operating speed. Therefore, the objective of the study is to determine the performance characteristics of centrifugal contactors with larger length-to-diameter ratios than those employed in the Savannah River units.

---

[2] D. S. Webster, C. L. Williamson, and J. F. Ward, "Flow Characteristics of a Circular Weir in a Centrifugal Field," USAEC Report DP-371 (June 1961).

[3] D. S. Webster, C. L. Williamson, and J. F. Ward, "Hydraulic Performance of a 5-inch Centrifugal Contactor," USAEC Report DP-370 (August 1962).

[4] A. T. Clark, Jr., "Performance of a 10-inch Centrifugal Contactor," USAEC Report DP-752 (September 1962).

[5] A. A. Kishbaugh, "Performance of a Multi-stage Centrifugal Contactor," USAEC Report DP-841 (October 1963).

[6] D. S. Webster, A. S. Jennings, A. A. Kishbaugh, and H. K. Bethmann, "Performance of Centrifugal Mixer-Settler in the Reprocessing of Nuclear Fuel," USAEC Report DP-MS-67-71 (October 1967).

[7] A. S. Jennings, "A Miniature Centrifugal Contactor," USAEC Report DP-680 (March 1962).

B. DESIGN OF CENTRIFUGAL CONTACTOR

A centrifugal contactor has been designed for testing and is currently being fabricated. The main components of the unit are shown in Fig. 1. The design is an adaptation of the Savannah River design with a restriction placed upon the stator diameter in order to maintain a critically favorable diameter for plutonium process solutions. A stator ID of 5 in. was determined to be critically safe for plutonium concentrations as high as 200 g/liter on the basis of data[8] on safe diameters of infinite water-reflected cylinders of $Pu(NO_3)_3$ solutions. It is not expected that Purex-type process flowsheets for which this type of contactor may be employed will approach a concentration of 200 g/liter. To add to the safety factor, the ID of the stator in the unit shown in Fig. 1 has been limited to 4 1/2 in.

In the unit shown, aqueous and organic phases enter the mixing chamber located below the 4-in.-OD hollow cylindrical rotor. The phases are mixed by a paddle attached to the end of the shaft that supports the rotor. Radial baffles located just above the mixing chamber direct the mixed phases into the bottom of the spinning rotor, where they are quickly accelerated to the bowl speed by four vertical vanes located inside the bowl. The phases are separated by centrifugal force as they move upward through the bowl and are discharged through ports near the top of the bowl. An air-controlled weir is used to adjust the position of the emulsion between the two phases, thereby preventing emulsion being discharged with either of the separated phases. This feature (which was developed at Savannah River) permits good operation over a range of flow rates, density ratios, and rotor speeds.

The rotor is supported only at the top in order to avoid problems that might be caused by bearings operating in corrosive solutions. Accord-

---

[8] H. K. Clark, "Handbook of Nuclear Safety," USAEC Report DP-532, Table IV.28, p. 442 (January 1961).

Figure 1

Experimental Long-Bowl Centrifugal Contactor

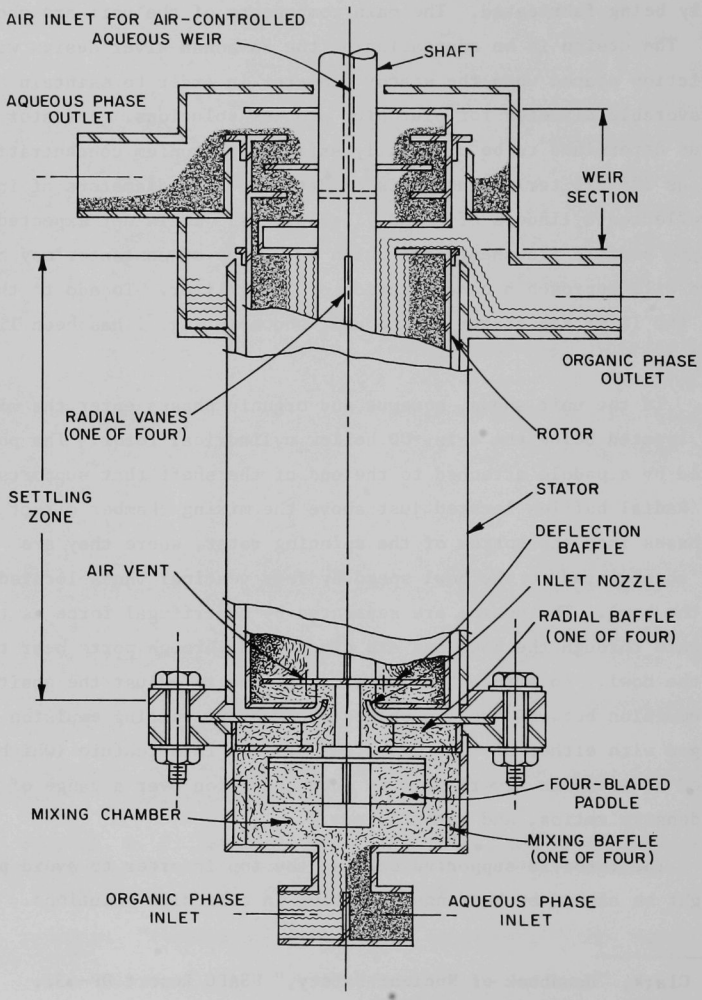

ingly, the length of the rotor and its operating speed are limited by the critical speed of the shaft and rotor assembly. At this speed any vibration resulting from rotor imbalance is strongly reinforced and can lead to excessive deflection, high stresses, and possible failure of the equipment. The spindle assembly which will support the rotor can accommodate a 1 1/4-in.-dia shaft. Calculations of critical speeds indicated that the rotor assembly would have a first critical speed of about 5400 rpm if the length of the rotor bowl were limited to 15 in. Since the generally recommended safe operating speed for rotating bodies is about 70% of the critical speed, operating speeds of about 3600 rpm should be permissible with the proposed rotor. The weir section occupies the upper 3 in. of the bowl length; the remaining 12 in. is available for use as a settling zone. The length-to-diameter ratio of three for the settling zone and the operating speed of 3600 rpm will extend the study of operating characteristics beyond the range covered by the Savannah River units, which have a settling-zone length-to-diameter ratio of about 1.3 and an operating speed of 1800 rpm.

The testing program to be carried out with the above contactor is designed to establish separating capacities with a nitric acid solution as the aqueous stream and tributylphosphate in refined kerosene or n-dodecane diluent as the organic stream. Performance data from these tests will be compared with performance data from tests of the Savannah River units. On the basis of the latter tests, a tentative relationship has been developed to correlate settling capacity with rotor speed, diameter, and length. Using this relationship, a settling capacity of about 12 gal/min is expected for the Argonne unit. The data from the proposed tests will be used to establish the validity of the relationship or to refine it and extend it to include the higher speeds and larger length-to-diameter ratio employed.

Present plans call for the procurement of a large commercial spindle which will permit tests of rotors having length-to-diameter ratios up to 5. Performance tests with such rotors will permit further extension

of the range of application of centrifugal contactors. It is anticipated that integration of the data from all the tests will form a basis for the design of centrifugal contactors which will have critically favorable geometry and which will be capable of flow rates up to about 20 gal/min.

In addition to tests with nitric acid and organic solvents, tests will be made with inactive uranium feed solutions using a Purex-type flowsheet to evaluate the mass-transfer efficiency of the contactor. One of the variables to be studied in these tests will be the effect of different geometries of mixing paddles. In the contactor design shown in Fig. 1, the bottom section can be removed to permit replacement of the mixing paddle with one of a different design. In addition, it is possible to remove the mixing paddle entirely and replace the bottom section of the contactor with a special housing. That housing would be equipped with a shaft seal to permit a mixing paddle to enter the bottom of the mixing chamber. This paddle would be driven by an independent motor drive, allowing investigation of the effects of operating the rotor bowl and the mixing paddle at different speeds.

Another physical modification of the contactor which can be made will permit it to be converted into an annular mixing unit. In this concept, there would be no mixing chamber or mixing paddle at the bottom of the unit. The aqueous and organic streams would be fed into openings at the side of the stator several inches below the collecting rings. The incoming streams would be mixed by the spinning rotor while moving downward in the annular space between the rotor and the stator. Small radial baffles on the bottom plate would direct the mixed phases into an orifice located at the bottom of the hollow rotor. Separation of phases within the rotor would take place as in the previously described design. It is expected that the spinning rotor will tend to center itself within the cylindrical stator in a manner similar to a rotating shaft supported by fluid bearings. Elimination of the mixing paddle at the bottom of the rotor will reduce the overall length of the rotor assembly and simplify construction.

Plastic models simulating the latter type of centrifugal contactor were tested, with water as a single phase, to measure pumping capacity and mixing-power input. On the basis of mixing-power input, it was predicted that adequate phase mixing could be achieved in the annular mixing chamber. A flow capacity of about 20 gal/min was predicted for a unit with a 4-in.-dia rotor. Since only water was used in these tests, the actual phase-separating capacity could not be measured in the test unit.

While the stainless steel centrifugal contactor is being fabricated, a plastic (acrylic) contactor of the annular type will be built and tested. This unit will have a mechanical weir to provide for independent discharge of the aqueous and organic streams. It can thus be used to test effectiveness of phase mixing and centrifugal phase separation. It will provide preliminary operating data which can be used as a basis for testing the stainless steel contactor when it is converted to the annular mixer design. If that design performs successfully, it will represent an improvement over the Savannah River design with respect to both simplification of construction and mechanical stability at high speed.

A facility has been built where experimental centrifugal contactors will be tested using various organic and aqueous streams. The facility is equipped with supply tanks for the aqueous and organic streams, pumps, constant-head tanks, and flowmeters. The spindle supporting the rotor will be driven through a belt by a DC motor to permit operation over a range of rotor speeds. The entire facility is enclosed in a ventilated hood to confine any organic or acid vapors released.

B